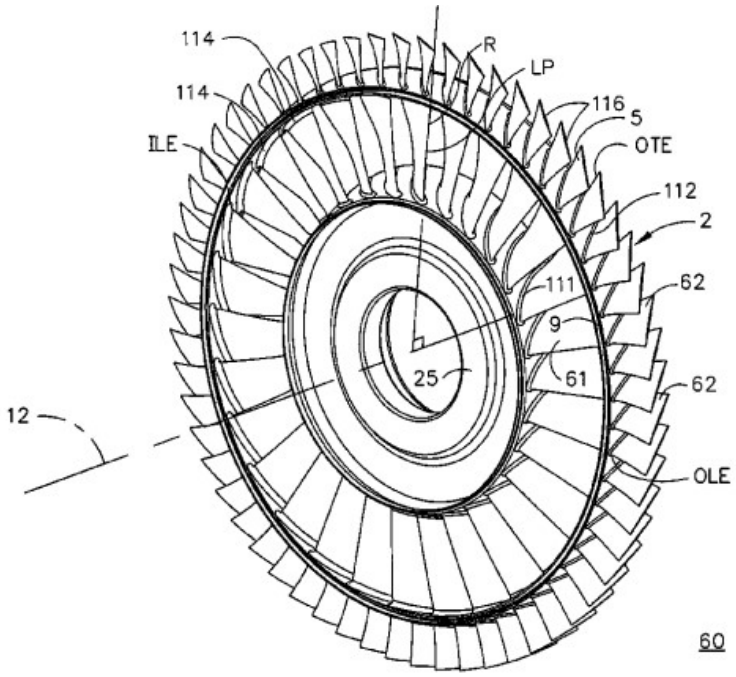

Low Bypass Ratio Variable Cycle Engine Concepts for High Speed Aircraft

Master's thesis in Sustainable Energy Systems, M.Sc.

ALI ALTAR INCEER

DEPARTMENT OF MECHANICS AND MARITIME SCIENCES

CHALMERS UNIVERSITY OF TECHNOLOGY
Gothenburg, Sweden 2022
www.chalmers.se

Master's thesis 2022

Low Bypass Ratio Variable Cycle Engine Concepts for High Speed Aircraft

ALI ALTAR INCEER

CHALMERS
UNIVERSITY OF TECHNOLOGY

Department of Mechanics and Maritime Sciences
Division of Fluid Dynamics
Chalmers University of Technology
Gothenburg, Sweden 2022

Low Bypass Ratio Variable Cycle Engine Concepts for High Speed Aircraft
ALI ALTAR INCEER

Supervisor: TOMAS GRÖNSTEDT, Department of Mechanics
and Maritime Sciences
Examiner: TOMAS GRÖNSTEDT, Department of Mechanics
and Maritime Sciences

Master's Thesis 2022
Department of Mechanics and Maritime Sciences
Division of Fluid Dynamics
Chalmers University of Technology
SE-412 96 Gothenburg
Telephone +46 31 772 1000

Cover: A technical drawing of a new engine component named "FLADE" from the respective patent file [9]

Typeset in LaTeX
Printed by Chalmers Reproservice
Gothenburg, Sweden 2022

An Informative Headline describing the Content of the Report
A Subtitle that can be Very Much Longer if Necessary
ALI ALTAR INCEER
Department of Mechanics and Maritime Sciences
Chalmers University of Technology

Abstract

There are many types of engines in aviation industry, among these turbofan engines are the most commonly used type. Low and medium bypass ratio engines are used predominantly in military aircraft and high bypass ratio ones are used in both civil and defence industries. Variable cycle engines (VCE) are advanced turbofan engines with multiple bypass ducts making them more efficient in a wider range of operating conditions. Adaptive cycle engines take it a step further by actively changing the fan pressure ratio (FPR) and making the engine performance even better. A new component recently patented called FLADE (Fan on bLADE) provides options such as having a third bypass duct hoping to further decrease SFC and improve efficiency. In this study, a FLADE'd engine will be studied to see if and how the addition of the FLADE affects the engine performance. An in-house built software called GESTPAN will be used for the analysis performed in this study. The fact that introducing new components to GESTPAN is relatively easy makes the adding of a FLADE component to models relatively easy. Although the initial intention was to study a triple by-pass ACE with FLADE, it was decided to concentrate the analysis on the comparison of a single bypass turbofan engine and a FLADE'd turbofan. Results show that the FLADE stream, when using a variable exhaust nozzle, is relatively resistant to choking. This means that it has the potential to alleviate spillage drag by increasing flow and decreasing specific thrust in low power conditions. This work indicates that the new FLADE'd engine has the potential to substantially increase propulsive efficiency of the FLADE stream. However, it is difficult to provide a substantial part of the thrust from this stream simple because of its lower specific thrust resulting in that the FLADE stream may not influence the overall engine performance to a great extent. This is because the kinetic energy contribution from the FLADE stream is almost negligible. Cruise analysis showed that adjusting the bypass ratio for the FLADE can result with considerable range benefits. Some of the other advantages of the FLADE could be that its stream can be used for cooling purposes such as a heat sink for cooling the turbine cooling air, which allows turbine inlet temperature (TIT) to be increased resulting with overall better engine performance.

Keywords: Turbofan, VCE(Variable cycle engine), ACE(Adaptive cycle engine), FLADE(Fan on bLADE), Breguet Range, GESTPAN, Choking, BPR(Bypass ratio), Cruise

List of Acronyms

Below is the list of acronyms that have been used throughout this thesis listed in alphabetical order:

AB	Afterburner
ACE	Adaptive Cycle Engine
BPR	Bypass ratio
CDFS	Core Driven Fan Stage
CPR	Critical Pressure Ratio
FLADE	Fan on bLADE
GE	General Electric
GESTPAN	GEneral Stationary and Transient Propulsion ANalysis
HPC	High Pressure Compressor
HPT	High Pressure Turbine
IFE	Inverted Flow Engine
IGV	Inlet Guide Vane
IPC	Intermediate Pressure Compressor
IPC	Intermediate Pressure Turbine
ISA	International Standard Atmosphere
LPC	Low Pressure Compressor
LPT	Low Pressure Turbine
NPR	Nozzle Pressure Ratio
OPR	Overall Pressure Ratio
P&W	Pratt and Whitney
SFC	Specific Fuel Consumption
SST	Supersonic Transport
TF	Turbofan
VCE	Variable Cycle Engine
VSCE	Variable Stream Control Engine

Nomenclature

Below is the nomenclature of indices, sets, parameters, and variables that have been used throughout this thesis.

Parameters

γ	Specific heat ratio
π	Pressure ratio
c_p	Specific heat
R	Gas constant

Variables

T	Temperature
M	Mach number
P	Pressure
C	Velocity
η	Efficiency
fa	fuel-air ratio
N	Rotational speed
A	Area
ρ	Density
$\dot{m}$	Mass flow
R_{Br}	Breguet Range
W	Weight

Contents

List of Figures

List of Tables

1
Introduction

Humanities fascination with flying goes back centuries if not millennia with folklore stories from all over the world. However, when humanity started to move really fast is when the Wright brothers performed the first controlled and sustained flight with a powered airplane in 1903 [1, 2]. Since then the aviation sector has improved greatly, especially after the invention of the jet engine by Frank Whittle in 1930 [3]. With the use of jet-engines it allowed planes to fly higher where the air is thinner (density is lower) and consequently the drag is lower. This made it possible to dramatically increase comfort during flight contributing to the rapid expansion of civil aviation.

1.1 Types of Jet Engines

These days there are many different types of jet engines used all over the aviation sector, for both commercial and military use. To put it simply, jet engines work by compressing the air with compressor(s), then fuel is mixed with the air and the fuel is burned causing the gases to increasing the temperature. The boost in energy is then used for expansion turning the turbines to provide power for the compressor(s). The excess energy left in the exhaust stream provides thrust for the aircraft (except in turbo-shaft engines which also uses a majority of the power to turn the shaft). Currently there are three main types of jet engines used for airplanes, these are the turboprop, the turbojet and the turbofan which can be seen in figure 1.1 [4].

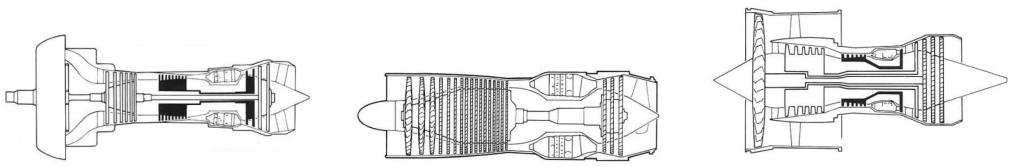

(A) (B) (C)

Figure 1.1: Engine layouts for (A) turboprop, (B) turbojet and (C) turbofan [4]

Turboprop usually fly at a low speed and altitude and for such missions they are quite efficient and more importantly they also have a low operation cost. The turbojet engine is a single stream engine which provides high levels of specific thrust but they have very low efficiency figures [5].

Turbofan engines can be seen as a middle ground between turbojet and turboprop engines, the development of two-stream turbofan engines started in 1960's and these engines offer greater cruise speeds at higher altitudes and have better efficiency than turbojet engines [6].

Turbofan engines range from low bypass ratio engines to high bypass ratio engines. High bypass variants are the preferred choice of engine for almost all commercial jetliners and low bypass variants are commonly used in military fighter aircraft.

An engine concept that can be favorable when it comes to military applications and/or supersonic transport is an engine called variable cycle engine (VCE). Research done on this engine type dates back to 1970's with the patent of VCE filed in 1977 [7]. These engines are still under development and being testing by industry leading manufacturers such as Pratt & Whitney and General Electric Aviation [8]. Varying from the initial patent the new engines have multiple bypass ducts offering a more powerful and more efficient engine at the same time.

In this study a relatively recent engine concept, a four-stream VCE, as in figure 1.2 will be studied. Over the years, several patents have been filed for a new engine component called FLADE (Fan on bLADE) [9, 10] which has opened up new possibilities for the propulsion system. One of which, is to have such an engine concept that has three bypass ducts as studied in this thesis work. This type of engine has been studied for decades, however due to high complexity of this engine type, especially with the addition of the FLADE, it can not be said that the technology is still under study. It should be noted that a lot of knowledge is believed to be available outside the range of public literature.

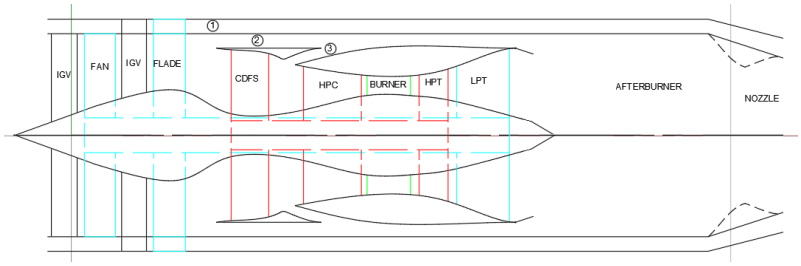

Figure 1.2: Engine layout for triple bypass turbofan

In this studying the goal is to see different engine modes for the given engine with different design points and mission plans (off-design points). The main objective of the study is to see if if the addition of FLADE and a totally separate by-pass for it on a given engine can yield higher efficiency values overall without hindering its performance when it comes to high thrust demanding mission points.

2

Background

As mentioned in the introduction, VCE is not new concept thus there is a respectable amount of research and testing done on it. This section of the report will go through both the theoretical background of this thesis work, as well as the literature review on the simulation and experiments done regarding the VCE.

2.1 Theoretical Background

In the theoretical background simple working cycle of a gas turbine will briefly be explained according to Gas Turbine Theory [11], also some concepts like corrected mass flow and mass flow compatibility will be discussed.

2.1.1 Basic Working Principles of a Turbojet Engine

As mentioned before a simple open-cycle for a gas turbine, a turbojet engine, includes some basic steps i.e. compression, combustion and expansion. The temperature (T) and entropy (S) diagram of such a cycle is given in the figure 2.1[1] below along with the respective engine layout.

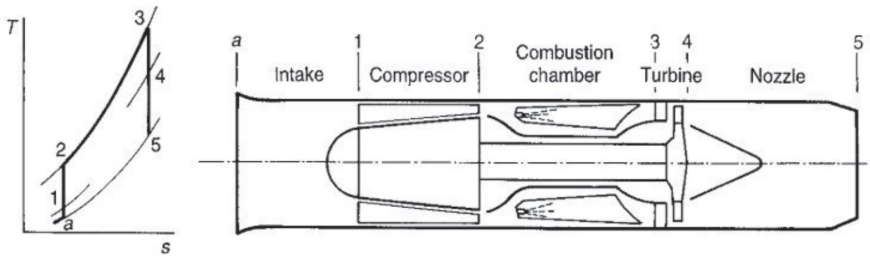

Figure 2.1: T-S diagram and the engine layout for a simple turbojet [11]

[1]In the section 2.1 index numbers mainly refer to station in figure2.1 unless the descriptive figure or text state otherwise.

While doing calculations for such a cycle the first thing to be done is to convert the atmospheric conditions that is read from the ISA tables to stagnation (total) conditions. This is done since over 100 m/s (360kph) [12] air can be considered as compressible and the temperature and pressure values needs to be adjusted. For an aircraft flying at flight velocity C_a the conversion to total conditions can be done as shown in equations (2.1) and (2.2).

$$\frac{T_0}{T_a} = 1 + \frac{\gamma - 1}{2} M^2 = 1 + \frac{C_a^2}{2c_{pa}T_a} \tag{2.1}$$

$$\frac{P_0}{P_a} = (1 + \frac{\gamma - 1}{2} M^2)^{\frac{\gamma}{\gamma - 1}} = (1 + \eta_i \frac{C_a^2}{2c_{pa}T_a})^{\frac{\gamma}{\gamma - 1}} \tag{2.2}$$

In both equations M represents the flight Mach Number and can be calculated with the equation (2.3), where C_a is the local speed of sound.

$$M = C_a/a = [a = \sqrt{\gamma RT}] = \frac{C_a}{\sqrt{\gamma RT}} \tag{2.3}$$

Air traveling through the inlet does not have a significant effect on the total conditions of it, thus $T_{0a} = T_{01}$ & $P_{0a} = P_{01}$. Air entering the engine is first compressed by the compressor, the increase in the pressure can be calculated using the pressure ratio of the compressor π. As can be seen from the figure 2.1, as the air travels along the compressor the temperature and pressure increase. The relations of pressure and temperature ratios before and after the compressor can be calculated as in equations (2.4) and (2.5).

$$P_{02} = P_{01}\pi \tag{2.4}$$

$$\frac{T_{02}}{T_{01}} = \frac{P_{02}}{P_{01}}^{\frac{1}{\eta_{poly}} \frac{\gamma_a - 1}{\gamma_a}} \tag{2.5}$$

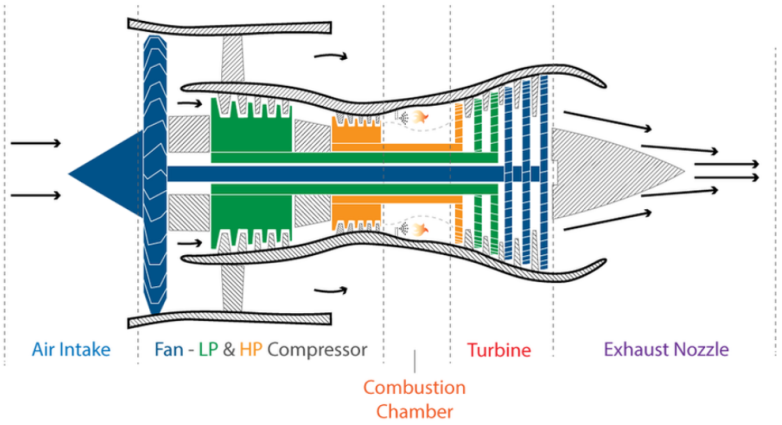

Figure 2.2: Three-spool engine layout [14]

In a modern jet engines there can be more than one compressor such as in the three-spool engine shown in figure 2.2 above. In such a case the pressure ratio between the inlet of the compressor and the inlet of the burner is not the π of a single compressor but rather the multiplication of the individual π's for each consecutive compressor component as in equation (2.6) below.

$$OPR = \pi_{Fan} \times \pi_{LPC} \times \pi_{HPC} \tag{2.6}$$

Air leaving the (last) compressor stage enters the combustor. The temperature of the exhaust gases leaving the combustor is limited by the metallurgic and cooling capability of the first turbine stage blades. In order to estimate the fuel/air ratio (fa) the temperature rise must be calculated and a chart such, such as in figure A.2, can be used. Also, the pressure drop along the combustor must be taken into account.

The main purpose of a turbine in a jet engine is to provide power for the compressor (s). The power need for the compressor can be calculated from the increase in enthalpy of the air (Δh). Since the enthalpy can be written as a function specific heat and temperature, as in $h = c_p T$, change of temperature can also be used for the calculation. Likewise, the power extraction can be estimated with the change in the enthalpy (or temperature change). Since fuel is added in the combustor the mass flow is increased. Change of the temperature of the exhaust gases are described by equation (2.7) below, where η_m is the mechanical efficiency of the shaft connecting the turbine and the compressor and c_{pg} is the specific heat of the exhaust gasses. When temperature ratio over the turbine is known the equation (2.5) can again be used but this time to get the pressure ratio.

$$(1 + fa)c_{pg}(T_{03} - T_{04}) = c_{pa}(T_{02} - T_{01})/\eta_m \tag{2.7}$$

Even though the pressure at the turbine outlet is considerably less than the pressure at the turbine inlet, it is still much greater than the ambient pressure. Therefore, the critical pressure ratio must be checked to understand if the nozzle is choked or not. Critical pressure ratio (CPR) and the nozzle pressure (NPR) can be calculated with equations (2.8) and (2.9) respectively.

$$\frac{P_{04}}{P_c} = \frac{1}{(1 - \frac{1}{\eta_j}\frac{\gamma_g - 1}{\gamma_g + 1})^{\frac{\gamma_g}{\gamma_g - 1}}} \tag{2.8}$$

$$NPR = P_{04}/P_a \tag{2.9}$$

In case the NPR is greater than CPR, then it can be said that the nozzle is choked. For a choked nozzle any further increase in the pressure will not effect the mass flow through the nozzle, the jet velocity of the gases are fixed at $M = 1$ and the nozzle static pressure P_5 will be equal to the critical pressure P_c. Since there is no active afterburner $T_{05} = T_{04}$ and the nozzle static temperature can then be calculated with equation (2.1). Since both the jet velocity in terms of Mach number and the static temperature of the jet is known, the jet velocity in terms of m/s can be calculated by equation (2.3). Lastly, the nozzle area can be calculated simply with $\dot{m}_{intake}(1 + fa) = \rho_5 C_5 A_5$. It is also possible to neglect the fuel mass flow since it is orders of magnitude smaller than the air mass flow from the inlet.

If the NPR is less than CPR the nozzle is not chocked thus $P_5 = P_a$ and the jet velocity need to be calculated. For this calculation the nozzle outlet static temperature is calculated first using the definition of the nozzle efficiency, as in equation (2.10). The calculation is started by multiplying both sides by the denominator of the right side and then dividing the left side by T_{04}. The temperature ratio on the left side $(\frac{T'_5}{T_{04}})$ can be converted into pressure ratio by using the equation (2.5) but since T'_5 is the temperature with 100% efficiency, the η_p term can be neglected.

$$\eta_{nozzle} = \frac{T_{04} - T'_5}{T_{04} - T_5} \tag{2.10}$$

With the static outlet temperature of the nozzle known, equation 2.11 can be used to get the jet velocity.

$$C_5 = \sqrt{2c_{pg}(T_{04} - T_5)} \tag{2.11}$$

Lastly the nozzle area required is calculated using the equation (2.12) below. It should be noted that the density ρ used in the equation should be obtained from the ideal gas relations, since it is quite dependent on the design of the engine cycle. f_{cc} and f_{ab} represent combustion chamber and afterburner air-to-fuel ratios respectively.

$$A_{Nozzle} = \frac{\dot{m}_{intake}(1 + fa_{cc})(1 + fa_{ab})}{\rho_{Nozzle} C_{Nozzle}} \tag{2.12}$$

2.1.1.1 Additional Principles

Almost exclusive to military jets, afterburners allow the engine to increase the thrust significantly with the penalty of increasing the specific fuel consumption. This efficiency drop will be explained in the next section 2.1.2). Afterburner work with the simple principle of dumping and burning more fuel after the outlet of the last turbine stage, hence the name afterburner. In the case of an afterburner, the thrust required sets the outlet temperature (T_{02}) since the jet velocity and thus the thrust is directly related to it. The the pressure drop along the afterburner is usually assumed as a design input, consequently the rest of the parameters are set being directly related to the pressure and the temperature. Since the resulting temperature is quite literally off-the-charts the 1^{st} law of thermodynamics can be used for first approximations. Equation (2.13) shows the 1^{st} law applied for the afterburner, in which T_{01}, T_{02} and T_{ref} corresponds to inlet and outlet total temperatures as well as an arbitrary reference temperature.

$$(1 + fa)c_{pg}(T_{02} - T_{ref}) + fa\Delta H_{ref} + c_{pa}(T_{ref} - T_{01}) + fc_{pf}(T_{ref} - T_f) = 0 \tag{2.13}$$

The remainder of the calculations are quite similar to the nozzle calculations, however, the nozzle area needed for an active afterburner is much greater. Thus when an afterburner is used, a variable area nozzle is also used.

The main difference between the turbojet and the turbofan is that in a turbofan engine some of the air is bypassed the engine core, the so-called bypass air. The ratio of air that is bypassed to the air going through the engine core is called the bypass ratio simply calculated by equation (2.14) below.

$$BPR = \frac{\dot{m}_{bypass}}{\dot{m}_{core}} \tag{2.14}$$

In an engine with multiple bypass ducts there are multiple bypass ratios and a total bypass ratio. For a triple bypass engine as in figure 2.3 below, the three bypass ratios are as given in equations (2.15), (2.16) and (2.17) respectively. Their bypass duct numbering are clarified by the encircled numbers in figure 2.3. Also, the total bypass ratio of the engine is given by equation (2.18) below.

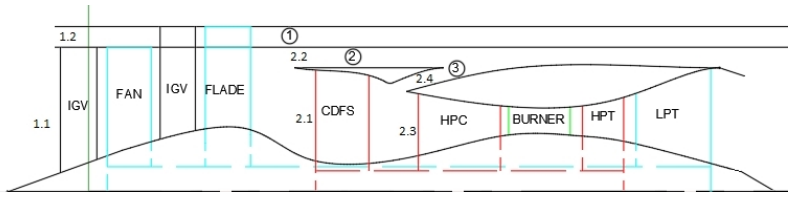

Figure 2.3: A triple bypass engine

$$BPR_1 = \frac{\dot{m}_{1.2}}{\dot{m}_{1.1}} \tag{2.15}$$

$$BPR_2 = \frac{\dot{m}_{2.2}}{\dot{m}_{2.1}} \tag{2.16}$$

$$BPR_3 = \frac{\dot{m}_{2.4}}{\dot{m}_{2.3}} \tag{2.17}$$

$$BPR_{Total} = \frac{\dot{m}_{1.2} + \dot{m}_{2.2} + \dot{m}_{2.4}}{\dot{m}_{2.3}} \tag{2.18}$$

2.1.2 Performance and off-design

Arguably the most important performance parameter of a jet engine regardless of the type is the net thrust output (F_{net}). Net thrust of an engine is simply calculated by subtracting momentum drag (F_D) from the gross thrust (F_G). F_D can be calculated using the intake mass flow and flight velocity as in equation (2.19). F_G can be calculated using equation (2.20), where the mass flow of the fuel in the main combustor and afterburner are included using the f_{cc} and f_{ab} parameters.

$$F_D = \dot{m}_{intake} C_a \tag{2.19}$$

$$F_G = \dot{m}_{intake}(1 + f_{cc})(1 + f_{ab})(C_j - C_a) + A_j(P_j - P_a) \tag{2.20}$$

An important variable metering engine fuel consumption is a parameter called specific fuel consumption (SFC), as can be seen from the equation (2.21). It quantifies how much fuel the engine uses for a given thrust.

$$SFC = \frac{\dot{m}_f}{F_{net}} \tag{2.21}$$

For a jet engine there are three types of efficiencies, these are the efficiency of energy conversion[2], propulsive efficiency and the overall efficiency. The efficiency of energy conversion describes how well the engine can turn primary energy from the fuel to kinetic energy of the gas stream and the propulsive efficiency describes how well the kinetic energy energy of the gas stream is converted into kinetic energy of the aircraft. Overall efficiency is the total efficiency calculation from primary energy of the fuel to kinetic energy of the aircraft. The definitions of the efficiency of energy conversion, propulsive efficiency and overall efficiencies are given in the equations (2.22), (2.23) and (2.24) below respectively, where $\dot{m}_f Q_{net,p}$ is the energy supplied by the fuel and $\dot{m}_f$ is the fuel mass flow. Lastly overall efficiency can be expressed as in (2.25) where in the equation $\eta_{combustion}$ can be neglected, as name suggests $\eta_{combustion}$ is the combustion efficiency which is usually in the range of 0.95-0.99.

$$\eta_e = \frac{\dot{m}(C_j^2 - C_a^2)}{2\dot{m}_f Q_{net,p}} \tag{2.22}$$

$$\eta_p = \frac{\dot{m}C_a(C_j - C_a)}{\dot{m}(C_a(C_j - C_a) + (C_j - C_a)^2/2)} = \frac{2}{1 + (C_j/C_a)} \tag{2.23}$$

$$\eta_o = \frac{\dot{m}C_a(C_j - C_a))}{\dot{m}_f Q_{net,p}} = \frac{FC_a}{\dot{m}_f Q_{net,p}} \tag{2.24}$$

$$\eta_o = \eta_e \times \eta_p \times \eta_{Combustion} \tag{2.25}$$

While making a cruise analysis, as in this thesis, the Breguet Range Equation (2.26) is a good option for estimating the range of the aircraft. The equation takes parameters into consideration such as energy contained in the fuel (h), the aerodynamic design of the aircraft with the drag on the aircraft (F_D), engine's efficiency of converting energy from the fuel to thrust (η_O) and weight of the aircraft at different points in time ($W_{Initial}$, W_{Final} and $F_L = W_{Current}$[3]). The equation can be written with SFC and flight speed as in the equation (2.27) [13].

$$R_{Br} = \frac{h}{g}\frac{F_L}{F_D}\eta_O \ln\frac{W_{Initial}}{W_{Final}} \tag{2.26}$$

$$R_{Br} = \frac{V(F_L/F_D)}{g \times SFC} \ln\frac{W_{Initial}}{W_{Final}} \tag{2.27}$$

[2]Efficiency of energy conversion is also commonly referred as the thermal efficiency (η_{th})

[3]Specific for cruise at the same altitude, not applicable for climb and descent phases of the flight

One of the important parameters when it comes to design and analysis of a gas turbine is the mass flow. Under some assumptions such, the flow being isentropic and compressible and the gas being calorically perfect the area Mach number relation can be expressed as in equation (2.28) and the mass flow for a choked flow can be expressed as in equation (2.29) [12]

$$(\frac{A}{A^*})^2 = \frac{1}{M^2}(\frac{2}{\gamma+1}(1+\frac{\gamma-1}{2}M^2))^{\frac{\gamma+1}{\gamma-1}} \tag{2.28}$$

$$\dot{m} = \frac{p_o A^*}{\sqrt{T_0}}\sqrt{\frac{\gamma}{R}(\frac{2}{\gamma+1})^{\frac{\gamma+1}{\gamma-1}}} \tag{2.29}$$

When these two equations are combined a mass flow function can be obtained as in equation (2.30). In this function the area calculated can be treated as the minimum flow area required to have a non-choked flow. Also, in such an equation the stagnation pressure and temperature would be decided by either the flight conditions i.e. flight velocity and altitude or both flight conditions and the engine components upstream of the component of interest. With stagnation temperature and pressure set and having values on the constant γ and R it can be said that mass flow is a function of flow Mach number and the flow area.

$$\frac{\dot{m}\sqrt{c_p T_0}}{P_0 A} = Q(\gamma, M) = \frac{\gamma}{\sqrt{\gamma-1}}M(1+\frac{\gamma-1}{2}M^2)^{-\frac{\gamma-1}{2(\gamma+1)}} \tag{2.30}$$

This function also sometimes called the Q-function when used in turbomachinery. When estimating flow areas along the jet engine stations, the Mach number should be taken as axial Mach number M_{ax}.

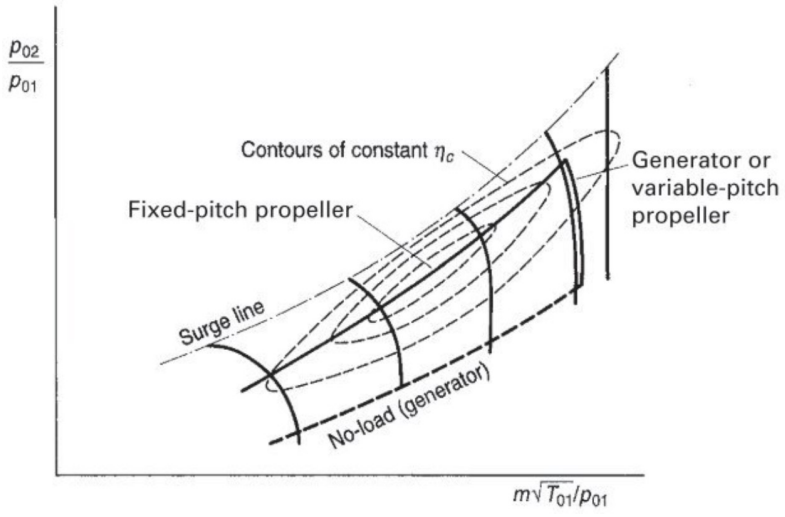

Figure 2.4: Compressor map and equilibrium running lines [11]

The figure 2.4 above shows the running lines plotted on a compressor map. A map is a graphical representation of the performance of a compressor component across its entire operating range. The vertical axis is the pressure ratio of the compressor (π) and the horizontal axis is the corrected mass flow through the compressor. Missing in the figure is the label for the almost vertical lines which indicate the corrected rotational speed of the compressor ($N/\sqrt{T_{01}}$). From this map expected efficiency of the compressor can be estimated with the parameters mentioned prior moreover, using the map it is possible to predict it if the compressor will be choking or surging. When a certain amount of power is required form the engine a single point need to be found along the constant speed line and this can only be done by a trial-and-error method, repeating the process several more time for different constant speed lines would give the equilibrium running line [11]. The equilibrium is obtained by matching conserved properties such as mass flows and shaft powers and at the same time varying the same number of iteration variables typically being compressor pressure ratios and rotational speeds.

Since the turbine and the compressor is connected to each other via a mechanical shaft it is easy to say that the both of them are rotating at the same rotational speed (N) thus a rotational speed compatibility can be formulated, as represented by equation (2.31). Also, using the conservation of mass a similar relation can be obtained for the corrected mass flow as in the equation (2.32) [11].

$$\frac{N}{\sqrt{T_{03}}} = \frac{N}{\sqrt{T_{01}}} \times \sqrt{\frac{T_{01}}{T_{03}}} \tag{2.31}$$

$$\frac{\dot{m}_3\sqrt{T_{03}}}{p_{03}} = \frac{\dot{m}_1\sqrt{T_{01}}}{p_{01}} \times \frac{p_{01}}{p_{02}} \times \frac{p_{02}}{p_{03}} \times \sqrt{\frac{T_{03}}{T_{01}}} \times \frac{\dot{m}_3}{\dot{m}_1} \tag{2.32}$$

If the mass flow of the fuel is to be neglected and there is no bypass ducts dividing the flow, the mass flow ratio term (fifth term n the right side) can also be neglected. p_{02}/p_{03} is the pressure drop in the combustion chamber and it is usually set externally.

2.2 Literature Review

As mentioned in Chapter 1, VCE research and development goes back to the 1970's. However one can argue that the variable cycle engine architecture goes all the way back to the 1950's with the J-58 engine designed for Lockheed SR-71 Blackbird. This engine may be the first variable cycle engine with relatively good performance at both subsonic and supersonic cruise. SR-71 and J-58 have many unique features and being first of its kind it features novel concepts such as suck-in doors for additional engine cooling at low speeds to bypass ducts that open only beyond a Mach=2.2 in order to increase the air flow that goes to afterburner. The schematics are presented in figure 2.5 (bypass ducts mentioned are not illustrated in the figure below).

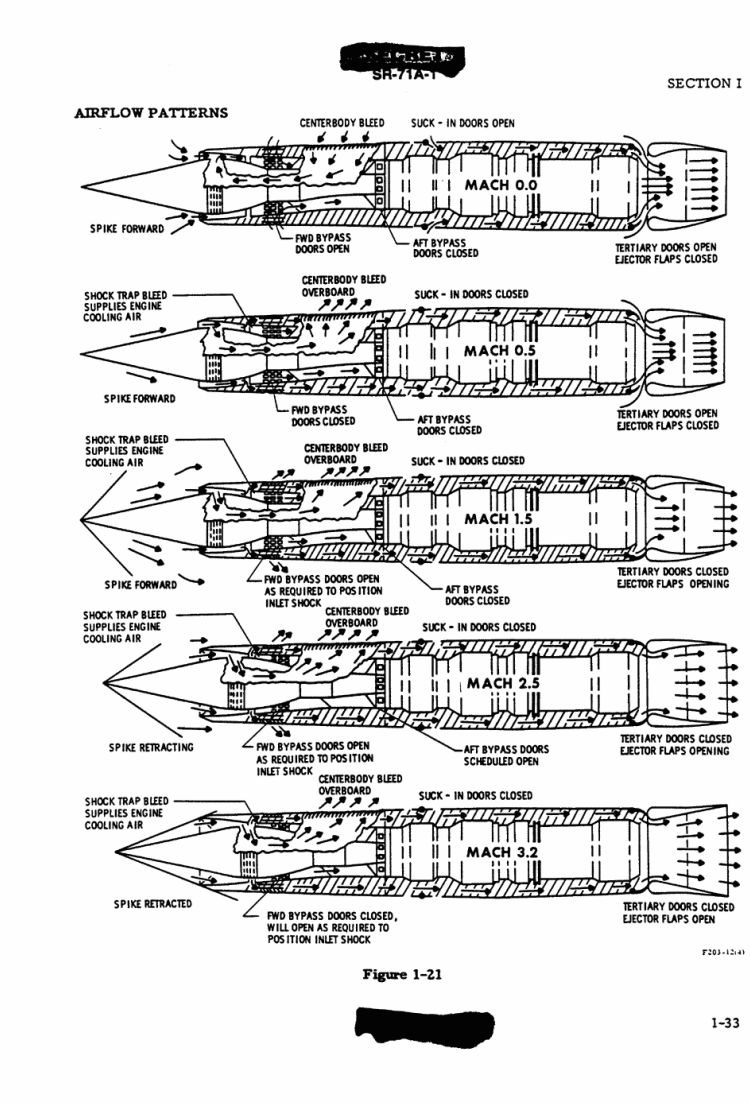

Figure 2.5: Airflow patterns for SR-71 engines [15]

As can be imagined VCE research is a relatively hot topic, and has been so for about four decades. There have been numerous papers published on it ranging from the US design efforts on supersonic transport rivalling the British/French Concord, to more military applications. In this section some highlights from the research will be mentioned.

In the original VCE patent file [7], it is said that VCE's can improve mixed mission performance, meaning when an aircraft is expected to perform things like subsonic cruise and supersonic cruise for military fighters or for supersonic transport vehicles like the Concord. It is also mentioned that this engine type can change between high specific thrust at supersonic speeds to low specific thrust at subsonic speeds. Furthermore, the patent claims that the fuel consumption of the aircraft over the given mission profile can be decreased. Lastly, in the patent file there are eight VCE layouts displayed with one or two bypass ducts.

As mentioned earlier USA attempted to design a supersonic transport plane with Boeing winning the design competition coming up with the 2707, see figure 2.6, to rival the Concord. During the development of this aircraft, a lot of improvements have been made including conceiving various VCE features. It is mentioned that VCE's can be a good option for second-generation SST's with emphasis on some requirements for VCE's such as co-annular nozzles, variable geometry fans and etc. [16].

Figure 2.6: Boeing 2707

During the development of the VCE's NASA granted contracts for both P&W and G.E. with specific requirements on emissions and jet noise. A way to reduce the jet noise is to have an adverse temperature gradient in the jet flow, i.e. the outer part of the jet flow being hotter than the inner part. G.E. and P&W came up with quite different engine layouts. P&W proposed a design with a single bypass duct using a duct burner for thrust augmentation. Also they suggested an ejector nozzle like in the SR-71. In order to accommodate changes in the duct burner, a variable-area duct-stream was used. Also, a variable-area nozzle for matching jet airflow and shaft speed with engine inlet flow was proposed Lastly, the aforementioned adverse temperature gradient has been obtained with the duct burner increasing outer bypass flow temperature. Due to these features the engine architecture is also called a variable-stream-control-engine (VSCE). On the other hand G.E. proposed the double bypass engine, a single bypass duct with the option of being fed from 2 separate points in the engine flow. Having this option allowed having either a low-energy stream in the bypass duct for subsonic cruise or essentially running the engine as a mixed-flow engine for supersonic cruise. Also, for the adverse temperature gradient GE's double bypass engine directs duct-flow inside to a nozzle on the exhaust cone. This engine style is also called inverted flow engine (IFE) [17].

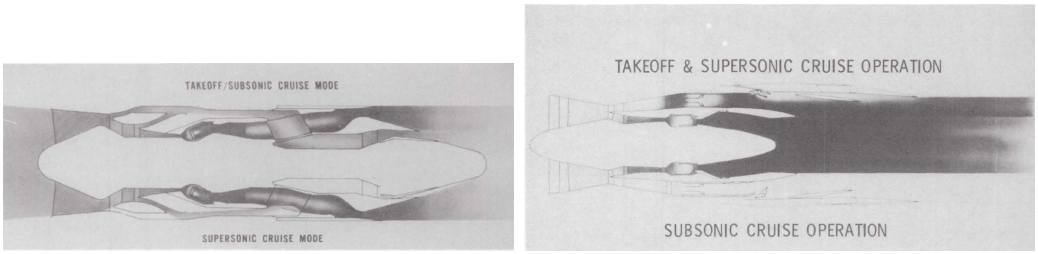

(A) (B)

Figure 2.7: Conceptual design for (A): GE IFE and (B): P&W VSCE [17]

As mentioned before one of the early ideas was to add a duct burner on one of the bypass ducts to increase thrust when needed. The effects of the duct burners have been researched thoroughly from the emissions to their aero-acoustics. When compared to the engine core flow the flow through the bypass duct is less uniform throughout the mission and it is more likely to change and affect the performance of the duct burner. In one of the research reports NASA therefore suggested that more work is required with experimental setups involving possible fan designs for both emissions perspective and noise [18]. In a later NASA report it was mentioned that duct burners have created some stability problems and wall temperatures were mentioned as a limiting factor. Perhaps equally important, a test rig for duct burner experiments exploded during testing [19]

As mentioned in the Chapter 1, several FLADE patents have been filed, more recently by Wadia et al. [9, 10]. However the first FLADE patent dates back to the 1970:s, see Fig. 2.8. In the patent a FLADE component, which appears to be quite similar to how the component is described in more recent patents is mentioned. It is explained that the FLADE can give the option of operating the engine in a wider BPR range and increase both the subsonic and the supersonic cruise performance [20].

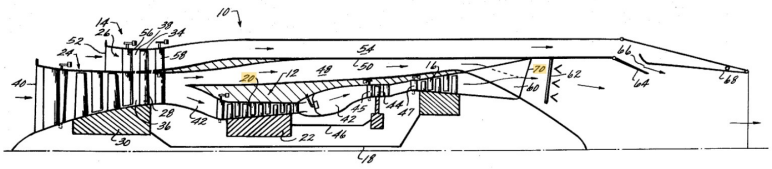

Figure 2.8: Two-spool variable cycle engine concept patent form 1976 [20]

Furthermore, G.E. filed another patent in 1995 which used a FLADE [21]. This patent is based on the technology already filed for the FLADE'd engine in 1976 and a hybrid rotor blade in 1993 [20, 22]. Hybrid rotor patents show the main idea behind the FLADE component, and shortly after filing this patent G.E. have also filed another patent for an engine with three bypass ducts and a FLADE [21]. In this patent they how this kind of an engine can possibly reduce the spillage drag occurring at the inlet and infrared radiation at the nozzle.

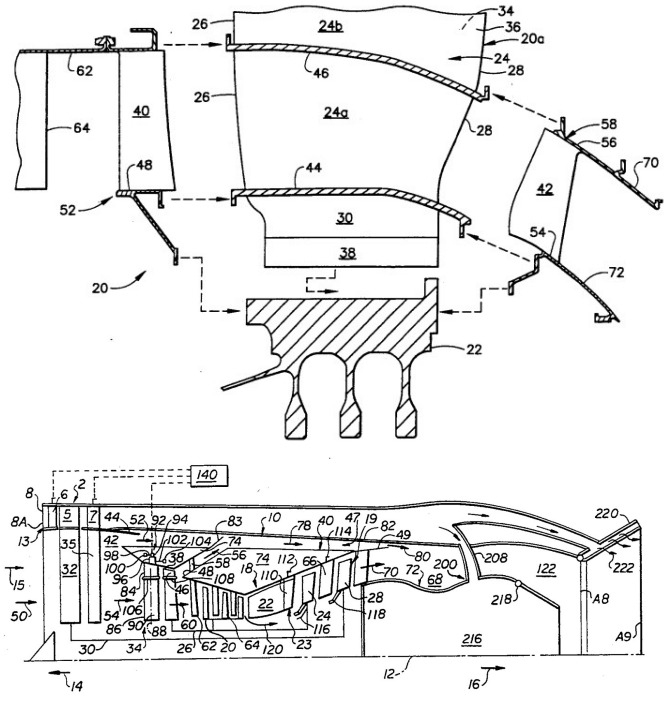

(A)

(B)

Figure 2.9: Hybrid rotor blade schematic (A) [22] (B)Engine layout for patented FLADE engine [21]

Spillage drag is a phenomenon that occurs when the engine is throttled down. The incoming airflow is then considerably greater than the flow that the engine can swallow. In such a case the engine cannot swallow the flow and incoming airflow would spill around the inlet until the aircraft slowed reducing the incoming flow per unit area. Unlike commercial airliners, military fighter planes need to perform combat maneuvers for which airflow spilling around the inlet can cause shock and vortex formations, which may induce additional drag on the aircraft. With spillage drag taken into affect, the SFC would increase substantially [6, 23].

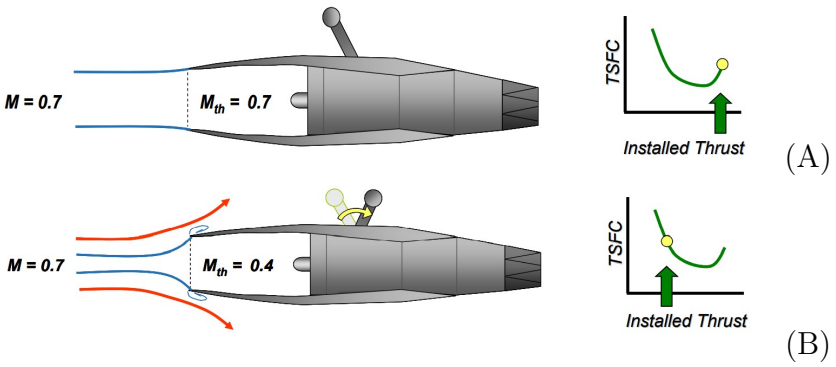

Figure 2.10: (A): Engine at cruise configuration. (B): Engine throttled down with spillage drag in affect [6].

Compared to a conventional turbojet or even a turbofan engine, VCE engines are inherently more resistant to spillage drag due to their different operating modes giving them much more flexibility. However, VCE's are not immune to spillage drag either. To some degree a type of VCE called the adaptive cycle engine (ACE) is being developed for this reason. The ACE engine patent was filed in 2009 and it was published in 2011 [24]. The ACE has an adjustable front fan stage which gives the ACE engine more flexibility compared with other VCE types and turbofans. The adjustable fan stage allows the engine overall pressure ratio to be controlled resulting in that the spillage drag can be reduced and the SFC can be decreased drastically [25, 26].

On the topic of in-flight engine behaviour adjustment, one of the technologies that has been quite beneficial when it comes to engine performance and efficiency is selective bleeding. A selective bleed engine can operate as a medium bypass engine at low flight speed and operate as a low bypass engine at high flight speeds [27]. With the selective bleeding; (Dry: Not-lit AB, not-augmented flight)

Table 2.1: Selective bleed VCE medium and low bypass ratio behaviours [28]

Medium bypass ratio	**Low bypass ratio**
good dry SFC	dry super-cruise
bypass from LP compressor exit	bypass from IP compressor exit
medium bypass ratio (1.0)	medium bypass ratio (0.4)
medium fan pressure ratio	high fan pressure ratio
two separate streams	mixed exhaust streams

One of the fortes of the software that will be used for this thesis work is control and optimization of selective bleeding. The software, is called GESTPAN (GEneral Stationary and Transient Propulsion ANalysis) [30, 29], and it will be discussed briefly in section 3.1.

One of the focal points of this thesis is to model the FLADE behavior and to predict what type of possible performance increase should be expected from this component. More specifically, it is studied how the FLADE could increase the engine performance in terms of efficiency while in subsonic cruise. As mentioned the FLADE is a relatively new component and limited research results exist in public literature. Existing work is mostly devoted to the whole ACE engine and very little work has been performed on investigating the active use of the FLADE.

3

Methods

In this chapter software used during this study will be explained along with the main principles and different operating conditions of the engine used. The main software used for this is GEneral Stationary and Transient Propulsion ANalysis (GESTPAN) [29] which has been created in Chalmers University of Technology in late 1990's. During the thesis work an interface for GESTPAN has been set up which can perform some manual work automatically to make the running and extracting of results less laborious. It should be mentioned it is not a mature tool and as of now it is only useful for VCE's and possibly ACE's .

3.1 GESTPAN

Initially, GESTPAN was developed to be a generalized tool for stationary and transient numeric simulations for gas turbine system performance hence the name, GEneral Stationary and Transient Propulsion ANalysis. After it was published many more functions have been introduced to GESTPAN, currently ranging from space launch vehicles and cryogenic liquid hydrogen tanks to more frequently used civil aircraft propulsion models. Some of the earliest cases that GESTPAN was used for was the optimization of the control of the transient performance of a selective bleed variable cycle engine during a mode switch [30].

It can be said that GESTPAN is a module based computational tool, which has predefined modules for components such as compressor, turbine, combustion chamber and many more which are connected together via a connector module. GESTPAN, being a module based tool, allows new modules to be introduced as needed with rather ease. The general structure of GESTPAN can be seen form the figure 3.1 below. Today, the JAVA GUI is not used but the FORTRAN 90 implementation is interfaced with Python or MATLAB.

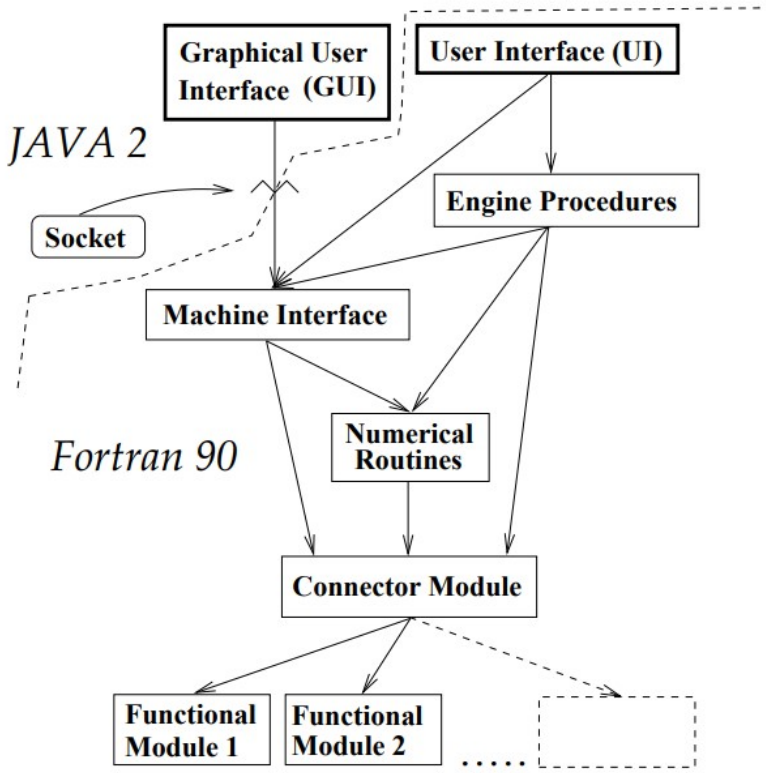

Figure 3.1: GESTPAN general structure [29]

Functional modules in GESTPAN i.e. compressor, turbine etc. can be adjusted and introduced as new technologies are developed and invented. A visual representation of a functional module is as in the figure 3.2 below. In the figure, input values are the output values coming from the upstream components such as gas temperature, pressure mass flow etc. Real and integer design parameters are fixed during off-design and transient calculations, however, some real design parameters are used as iteration parameters during design calculations. A brief explanation of what constitutes an iteration variable is, that this parameter is not defined by the user in any way. GESTPAN can automatically detect such parameters and it goes through every possible value for such a variable.

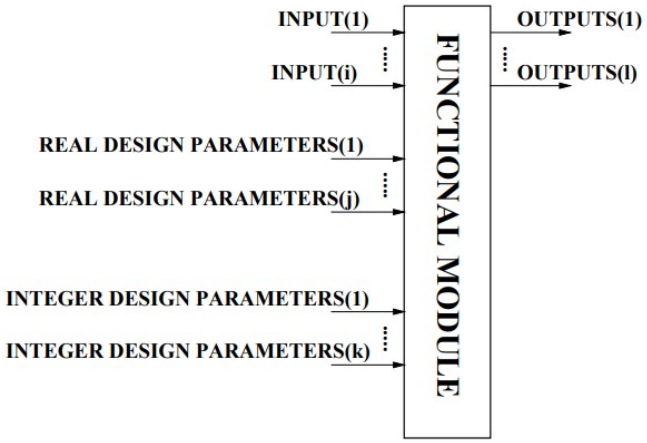

Figure 3.2: GESTPAN functional module [29]

It can be seen from figure 3.1 that GESTPAN has a graphical user interface (GUI) with JAVA2, however, it is also possible to access through the windows command prompt. When the windows command prompt is used the required input file is a text (.txt) file written in a certain manner and the output file generated is again a text file (s). Figure 3.3 shows the GESTPAN UI using the windows command prompt.

Figure 3.3: GESTPAN UI for Command Prompt

Another one of GESTPAN's functionalities is that for given components it can show where the design point and any off-design point is relative to the component map such as compressor. As mentioned in Chapter 2.1.2 these maps are crucial for understanding how much headroom there is until a stall or a choke occurs in the engine which hinders the performance of it.

When GESTPAN is performing an off-design calculation it goes from design point to off-design point (or from one off-design point to the next design point) in a certain number of steps. These step are called embedding points and the software checks multiple residuals on all of the embedding points. It gives the simulation (at the particular off-design point) for the last embedding point only. It has been seen that a large number of embedding steps make the simulation slow and actually more

prone to failure, therefore by default GESTPAN works with 20 embedding points.

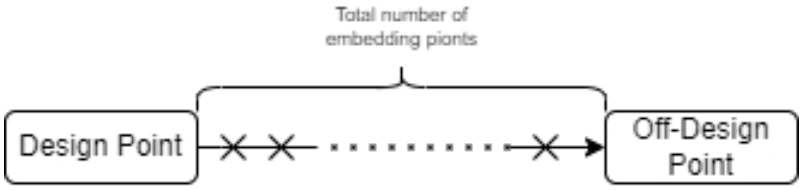

Figure 3.4: Embedding points

For a better understanding of GESTPAN it is suggested for reader to go through "Development of methods for analysis and optimization of complex jet engine systems" by Tomas Grönstedt [29].

3.2 MATLAB interface for GESTPAN

During the project a MATLAB interface to be used along GESTPAN was created. The main functionality of this interface was to allow a user with minimal knowledge of GESTPAN to use basic parameter estimation functionality of GESTPAN, which provides estimation for parameters such as thermal efficiency, propulsive efficiency along with many other output variables. Other than this, the interface allows users to change/add the following input parameters to the input text file.

- Changing module parameters i.e. compressor (s) pressure ratio
- Design point parameters i.e. bypass ratios of different streams
- Mission/off-design points either with manual entry or defining the mission over Excel

Moreover, if needed these changes can be done as a value range instead of a single value. When the user wants to try a range of values the interface makes it so that all possible combinations for the module parameters have been tried for all of the mission point. The interface gives three options for mission point entry for the simulation:

- Import mission points from 'mission.xlsx' file created by the interface.
- Adding mission points by hand through the MATLAB interface.
- Using the mission profile from the original input text file.

Currently, design point changes cannot try every possible combination and runs the simulation for a single range of design point parameter. After the user inputs the values or ranges required for the model the interface automatically runs the inputs in the above mentioned manner. In the end of the simulation the user is presented with the option whether the combinations evaluated should be written into an excel

file or not.

By the nature of GESTPAN and the interface all the output files are named the same an since a sizable number of simulations cases have been performed rapidly it is not efficient for user to manually pause the run and make a copy of the output file. Therefore, the interface automatically sorts and stores the output files. A general working schematic of the interface is as in the figure 3.5 below.

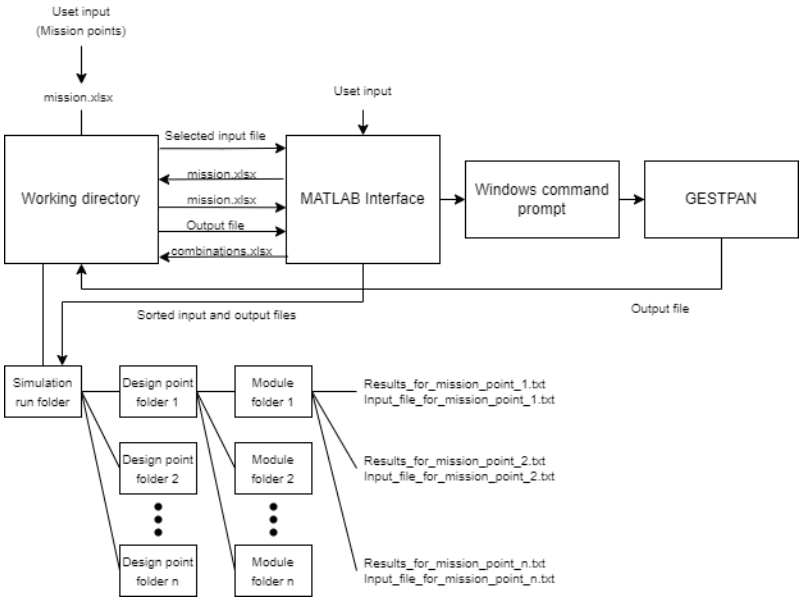

Figure 3.5: MATLAB interface working diagram

At the end of the interface script the user has the option of running a separate result processing script which gives the option of sorting the results. Also, the user can generate plots of any parameter needed from any module needed from both design and off-design points.

It needs to be mentioned that neither this interface nor the result processing script is bug-proof and both can greatly benefit from some improvements regarding the robustness and flexibility. In case it is needed further work on both scripts can improve overall analysis times.

3.3 Engine types studied

As mentioned in Chapter 1 the goal of this study is to see if the addition of the FLADE and the third bypass duct can yield better performance values. Ultimately the FLADE is hoped to put in a double bypass ACE engine making it a triple bypass ACE as in the figure 3.6 below.

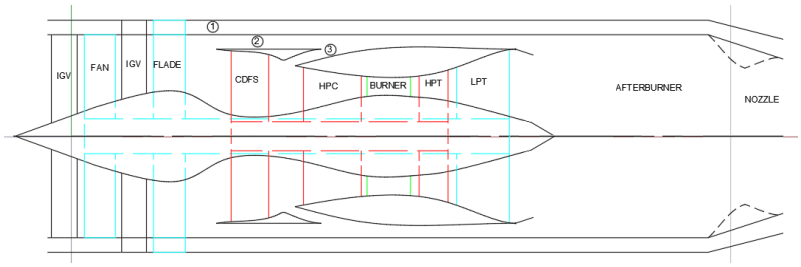

Figure 3.6: Triple bypass ACE engine with FLADE

It is known that an ACE has many aspects that need to be adjusted for a proper optimization. Furthermore, for the consistency of the analysis of how the FLADE and the new bypass would affect the results needs to be compared to a recent ACE model with a double bypass that has been modelled GESTPAN. Since there is no literature on such an analysis it has been determined that it would be more appropriate to study a low single bypass turbofan engine with a FLADE and second-bypass would be added separately in order to have a more direct comparison of the two architectures.

Recently the research group published a paper about power extraction from a high-pressure turbine (HPT) of a turbofan [31]. The paper examines the engine performance both with and without power extraction. The variant without power extraction will be used as a basis for this work. The layout of both the engines studied in the aforementioned paper and the FLADE added variant of it, as presented in the figure 3.7 below and also in table 3.1, show the specifications of the FLADE/FLADE stream.

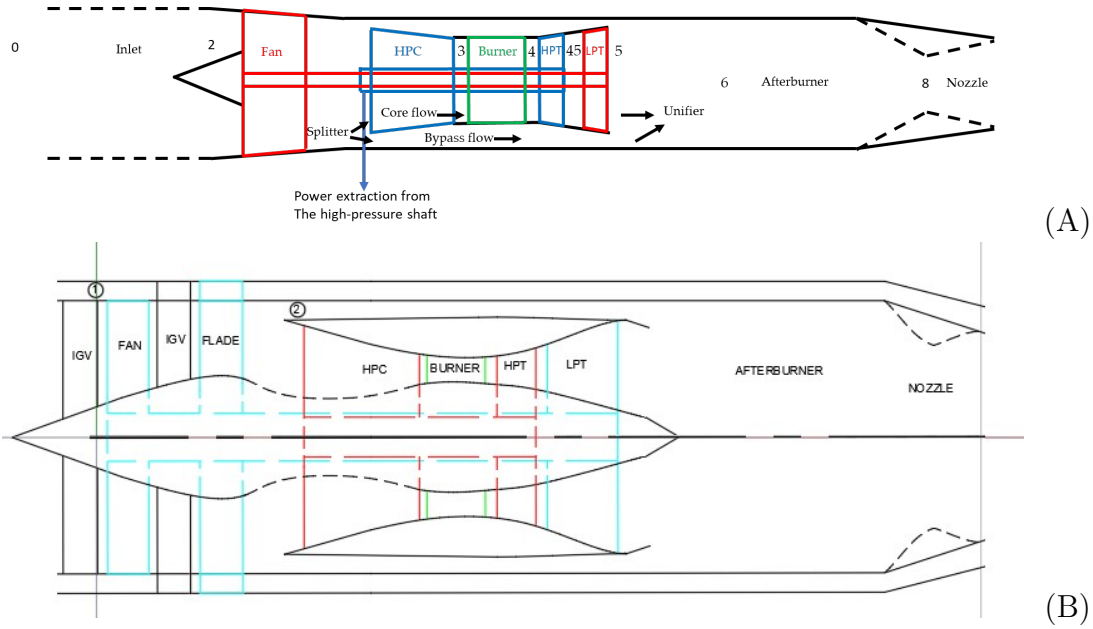

Figure 3.7: Engine layouts for (A) the low single bypass ratio turbofan [31] and (B) the low single bypass ratio turbofan **with** added FLADE and FLADE stream

Table 3.1: FLADE and FLADE stream specifications

BPR	0.1
FPR	2.0
η_p	0.89

VCE:s select the cycle mode depending on the flight conditions for the aircraft. In this study we analyse four operating modes:

- Range extended turbofan mode → In this mode both bypass ducts are open.
- Only FLADE → In this mode only the FLADE bypass (Duct 1) is open and bypass after the fan (Duct 2) is closed.
- Turbofan mode → In this mode the FLADE bypass is closed and the bypass after the fan is open. The engine operates very much like a low single bypass ratio turbofan engine.
- All closed mode → In this mode both bypass ducts are closed and the engine operates like a turbojet engine.

In this study not all four operation modes will be studied. Mode 2 and mode 4 will not be taken into consideration due to following reasons:

- Only FLADE → When the inner bypass duct (duct 2) is closed more of the air entering the engine is compressed, resulting in that the core stream jet kinetic energy is much higher than the FLADE stream kinetic energy. This results in that the contribution from that stream being negligible resulting in a higher SFC. For flade jet exit velocities very close to the flight speed, the net thrust is close to zero and the flade stream is mostly generating additional loss.
- All-closed mode → As established in Chapter 1, turbojet engines can produce very high levels of specific thrust but they would be inefficient in cruise operation. The main goal of this work is to see the effect of the addition of a FLADE, in particular for increasing cruise efficiency. The all-closed mode neither uses the FLADE nor does it give competitive performance in cruise. For these reasons this mode is not studied herein.

The main mode that will be studied here is mode 1, the range extended turbofan mode. As this mode is able to generate high efficiency cruise performance, it will be compared to the results of a conventional turbofan engine, mode 3.

3.4 Analysis plan

The mission plan executed for the power extraction analysis is as in the table 3.2 below. In the mission plan below it can be seen that at the subsonic cruise point (point 7) the thrust is low relative to the Mach number. Therefore, it can be said that at that point the engine is throttling, and as previously established there is a risk that the engine receives more incoming airflow than needed resulting in spillage

drag. In addition, charging the inlet from the intake ram, the pressure in the FLADE exhaust may increase. If the nozzle was designed unchoked due to a low speed and low design FPR of the FLADE, an increase in speed may charge the exhaust nozzle causing the mass flow through the FLADE to increase. This may push the FLADE into choke.

Table 3.2: Mission executed for power extraction analysis [31]

Point	Mission phase	Required Net Thrust (kN)	Altitude (m)	Mach No
1	Warm-up (AB not-lit)	66.0	610	0.0
2	Runway acceleration (AB lit)	110.7	610	0.1
3	Runway acceleration (AB lit)	112.9	610	0.18
4	Flight acceleration (AB lit)	127.3	610	0.44
5	Climb and acceleration (AB lit)	127.8	2743	0.775
6	Climb and acceleration (AB lit)	78.9	7010	0.9
7	Sub-sonic cruise (AB not-lit)	12.4	9144	0.9
8	Sustained turn (AB lit)	100.6	9144	1.6
9	Sustained turn (AB lit)	53.2	9144	0.9
10	Escape dash (AB lit)	113.9	9144	2.0

In addition to the mission plan in table 3.2 above, a subsonic cruise performance analysis will be done. The Mach numbers and thrust requirements[1] for the cruise analysis are found in table 3.3 below. This study will be done at the mission point 7 defined in table 3.2.

Table 3.3: Mach Number and thrust values for cruise analysis

Mach No	Thrust[N]
0.45	18537
0.5	19210
0.55	19870
0.6	20747
0.65	21606
0.7	22692
0.75	24201
0.8	26060
0.85	28621
0.9	32295

For the analysis of how the addition of the FLADE would affect the engine performance, the following analysis will be conducted;

[1]The thrust values in table 3.2 given in table 3.3 are for a similar aircraft.

- Choking analysis → Under which circumstances does the FLADE choke.
- FLADE performance → what is the efficiency levels of the FLADE stream and how much kinetic energy does it provide for thrust development.
- Engine comparison → Validation of the Turbofan model and comparison between the Extended Range model and the turbofan model. Also, subsonic cruise performance of the engines while testing different BPR values for the FLADE stream will be undertaken.

4
Results

In the previous chapters it has been explained how an added FLADE stream can help with the propulsive efficiency and spillage drag. Also, it has been stated that the spillage drag is mainly caused by by a mismatch between the engine mass flow and the aircraft operation. In this chapter it will first be shown under which conditions the FLADE stream can be choked and secondly how the new FLADED engine compare to the conventional turbofan engine.

4.1 Choking at Off-Design point

The Q-function shown in the equation (2.30) describes that the corrected mass flow is a function of Mach number and flow area for a given flight altitude. Also, since all the analysis performed is for aircraft flying on planet Earth, γ and R will be taken as constant. With the stated assumption it can be determined whether the flow will be choked or not from the flight Mach Number and flow/nozzle area.

For the choking analysis the aforementioned point 7 from [31] will be used, with the exception being that the altitude will be set to 9144 m. The reason for this change is that during a discussion with the author, it became clear that point 7 was intended to be flown at 9144 m, something that can be confirmed from the performance table in the appendix of [31]. During the simulation it has been observed that the FLADE stream is more sensitive to changes in design conditions for the new off-design altitude. For this reason, the FLADE design pressure ratio dependence has been analysed at both altitudes and an altitude and choking dependency study has been performed.

4.1.1 Pressure Ratio Relation

In Chapter 2.1.1 concepts like pressure and temperature ratio across a compressor has been introduced, see equations (2.4) and (2.5). Since the FLADE is essentially a compressor the same relations can be used to approximate its performance as for other compressor components. The left-hand side of the Q-function in equation (2.30) is very much like a corrected mass flow term. Thus, mass flow compatibility in equation (2.32) can be applied and in the resulting equation temperature ratios and pressure ratios can be substituted using the relations mentioned before.

The expression represented by equation (4.1) can then be obtained.

$$\frac{\dot{m}_1\sqrt{c_pT_{01}}}{P_{01}A_1} = \frac{\dot{m}_2\sqrt{c_pT_{02}}}{P_{02}A_2} \times \frac{A_2}{A_1} \times \frac{1}{\pi_{FLADE}} \times \sqrt{\pi_{FLADE}^{\frac{1}{\eta}\frac{\gamma-1}{\gamma}}} \tag{4.1}$$

From this expression it can be seen that the changes done on the FPR has a direct impact on the corrected mass flow and thus it will influence how prone the engine is to choking in the FLADE stream.

4.1.1.1 Analysis At Flight Level 7010 m

From figure 4.1 it can be seen that with the increase of the of FPR the choking margin of the FLADE stream increases. However, having a too high FPR such as 2.5 on a single turbomachinery stage can be seen as unrealistic.

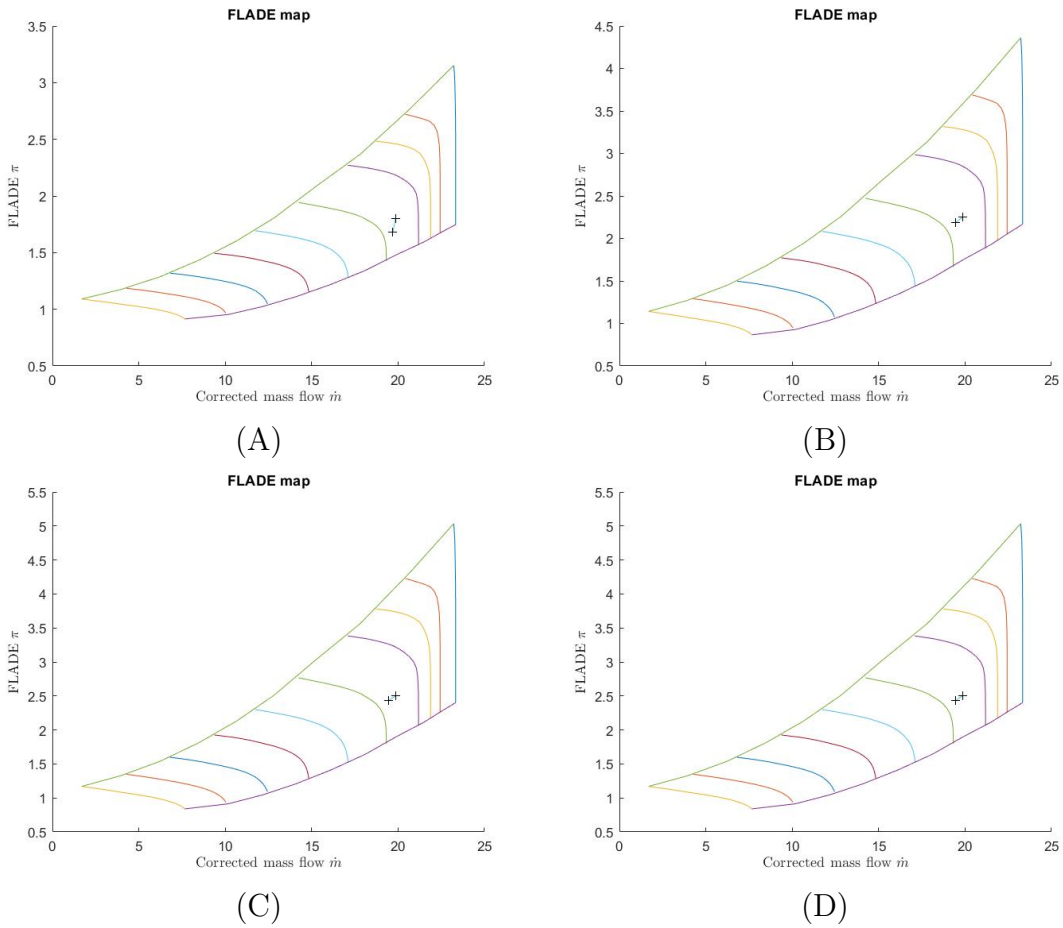

Figure 4.1: FLADE maps for (A) FPR=1.75, (B) FPR=2.0, (C) FPR=2.25 and (D) FPR=2.5

4.1.1.2 Analysis At Flight Level 9144 m

As mentioned prior altitude simulations done at flight level 9144 m have shown that the FLADE steam is more sensitive relative to flight level 7010m. Figure 4.2 shows that the choking margins for the FLADE stream are reduced noticeably with the change of the flight altitude.

Unlike the previous simulation the FLADE stream begins choking when the FPR value drops below 1.79 whereas at flight altitude 7010m FPR of 1.75 has been simulated without any choking issue.

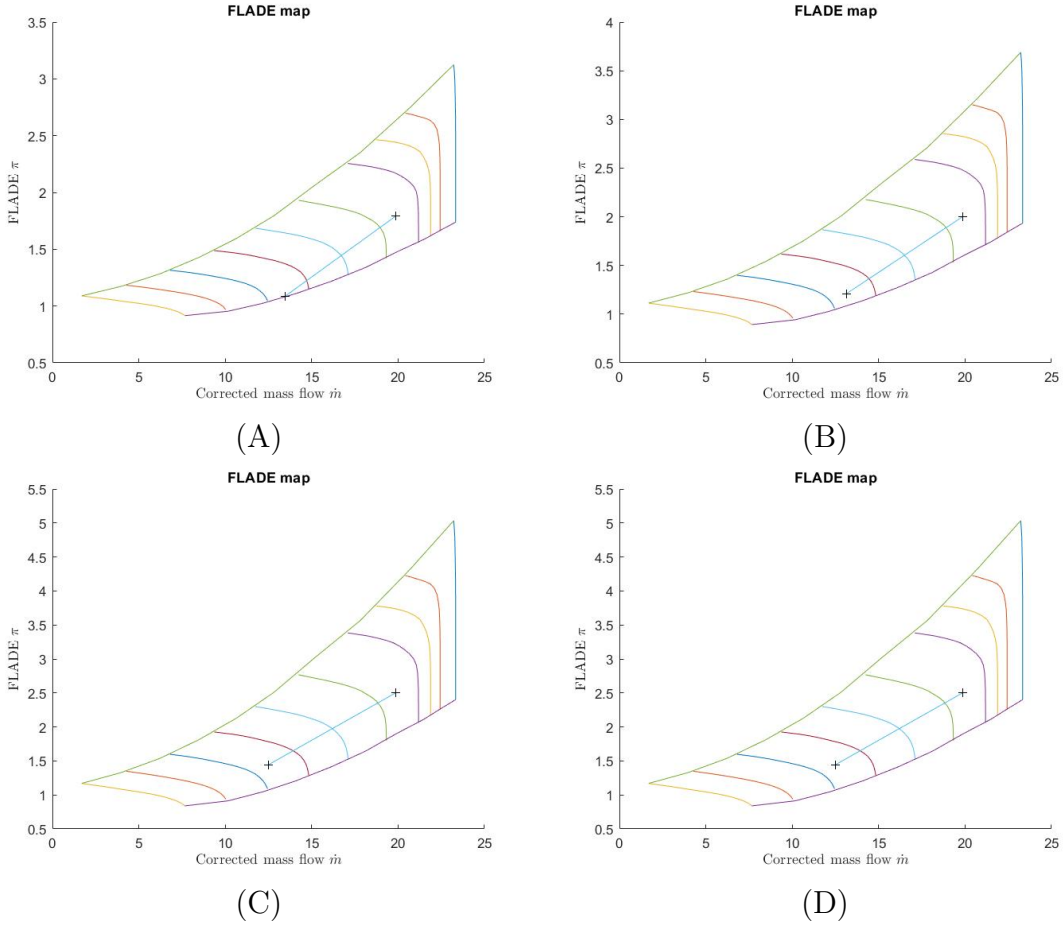

Figure 4.2: FLADE maps for (A) FPR=1.79, (B) FPR=2.0, (C) FPR=2.25 and (D) FPR=2.5

This notable sensitivity to design conditions is likely to be reduced if the FLADE BPR is increased from 0.1 to higher values. Also, it is possible to control the proximity to choke/surge using a variable exhaust nozzle in the FLADE stream.

4.1.1.3 FLADE Map Change with FPR and Altitude

As it can be noticed from the figures 4.1 and 4.2 that with the increase of FPR the operable area of the map gets wider. The change can be seen more visibly from

figure 4.3 below. Also, it can be seen from figure 4.3 that with the change of the flight altitude, the outline of the FLADE maps do not change.

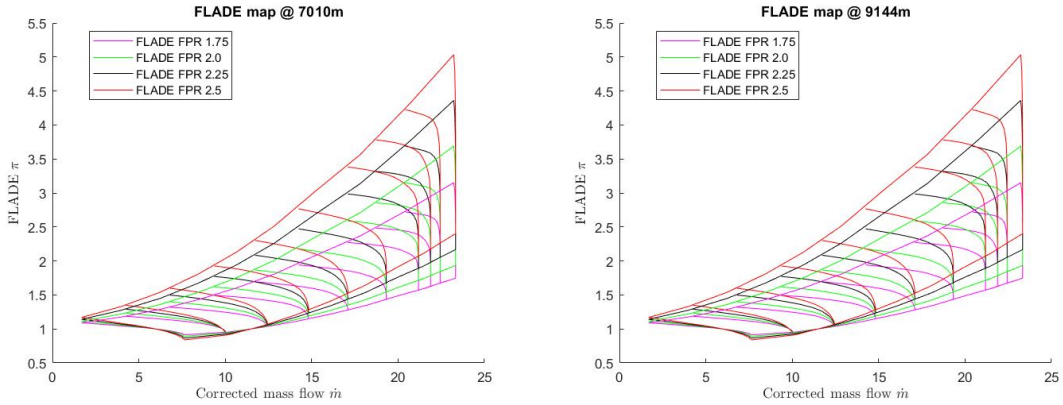

(A) (B)

Figure 4.3: Combined FLADE maps for flight altitude (A)7010m and (B)9144m

These results further emphasise the claim of having a larger FPR gives more choking margin and operational flexibility to the engine.

4.1.2 Further Altitude Relations

As presented in the figure below, as the altitude is increased from 7000 m to 10000 m the off-design point gets closer to the choking condition. However, as the altitude is increased beyond 12000 m and eventually to 15000m the choking tendency of the off-design point got smaller.

This may look odd at first, but reviewing the the ISA tables A.1 it is visible that as the altitude increases both temperature and pressure drop. Yet, the changes are not proportional and after some point the pressure keeps dropping while the temperature stabilizes around 216.7K until 20000m. From this, it can be said that around 9000 m, under the assumed conditions, is where the FLADE stream is most prone to choking.

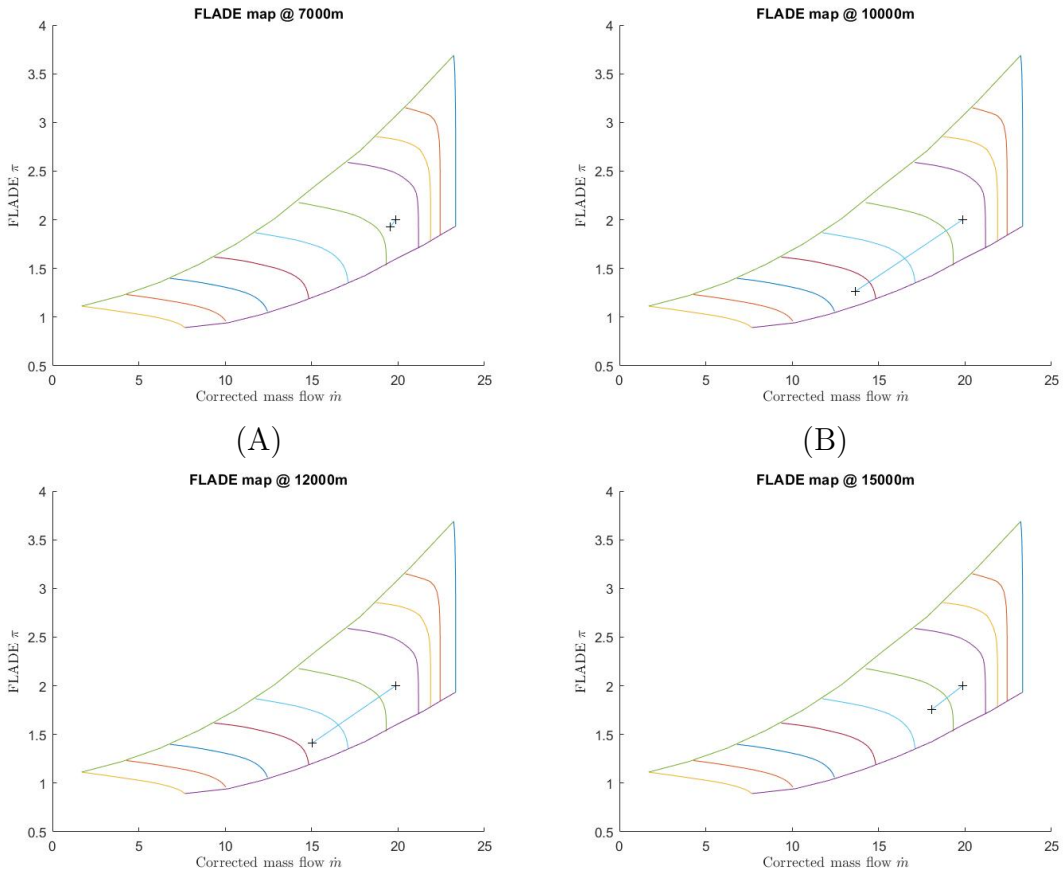

Figure 4.4: FLADE maps for altitudes (A) 7000m, (B) 10000m, (C) 12000m and (D) 15000m

4.1.3 Mach Number Relation

As presented in the figure 4.5 with the reduction of the Mach Number, the off-design point moves away from choking. Effectively, increased ram pressure ratio has the same influence as increased FLADE pressure ratio. However, it can also be seen that the changes across the different Mach Numbers are relatively small when compared to the effects of the other two factors, i.e. FPR and altitude.

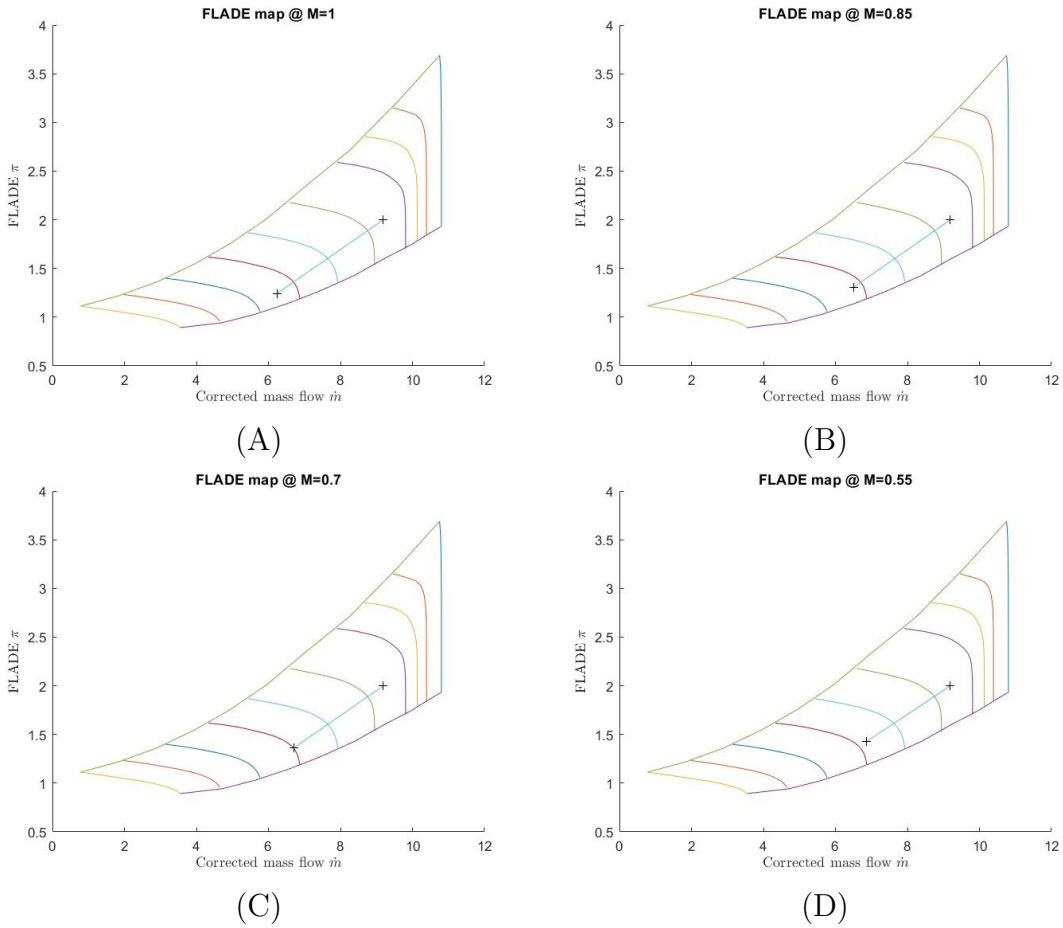

Figure 4.5: FLADE maps for Mach Numbers (A) M=1.0, (B) M=0.85, (C) M=0.7 and (D) M=0.55

4.2 FLADE Performance

As stated some analysis has been done for the purpose of seeing the performance of the FLADE stream, i.e. the efficiency of the FLADE component and the kinetic energy provided by the FLADE stream. It is expected to have efficiency figures close to the design efficiency of the compressor stage, while kinetic energy contribution from FLADE is expected to be substantially lower than the kinetic energy from the core stream due to the low BPR.

4.2.1 FLADE Efficiency

As it was predicted the efficiency of the FLADE is quite similar to the design polytropic efficiency as presented in table 4.1. For the mission plan the efficiency never dropped under 0.875 which is quite close to design efficiency. However for the cruise analysis it can be seen that with the increase of the Mach number up to $M = 0.85$, the efficiency of the FLADE did increase.It should be noted that these trends depend heavily on where in the map that the design point is placed.

Table 4.1: FLADE stream efficiency for both mission plan and cruise analysis

Mission plan	Cruise Analysis
η_{poly}	η_{poly}
0.890	0.869
0.887	0.879
0.887	0.88
0.888	0.880
0.888	0.881
0.883	0.882
0.808	0.884
0.890	0.884
0.886	0.885
0.875	0.883

4.2.2 FLADE Stream Kinetic Energy Contribution

It was expected that when the kinetic energy from the FLADE is compared with the core stream it would be substantially lower than that of the core stream due to the low BPR. However, the results in table 4.2 show that the ratio of the FLADE stream kinetic energy to the core stream kinetic energy is so low that the FLADE stream kinetic energy can be neglected in some points, i.e. mission plan point 5, 6, 7 and 9 and cruise analysis point 10. With that being said, the ratio is relatively high for mission points 1, 2 and 3, and cruise analysis point 1, 2 and 3 which indicates that lower flight speeds is where the FLADE is more useful.

Table 4.2: Core and FLADE stream kinetic energy production

Mission Plan		Cruise Analysis	
$W_{kin,core}$ [kJ/s]	$W_{kin,FLADE}$ [kJ/s]	$W_{kin,core}$ [kJ/s]	$W_{kin,FLADE}$ [kJ/s]
26636.7628	348.8815	5497.595	37.6346
63855.6927	385.6701	5692.155	36.7251
65283.4520	352.3435	5875.628	32.0268
70346.7206	202.1337	6145.375	27.4556
67163.5601	47.0174	6401.476	23.0126
43813.9205	13.8038	6748.462	18.9511
2559.8677	1.9781	7276.548	15.3605
58602.8165	77.3993	7962.209	12.1028
28405.9031	6.1016	8975.857	9.2902
56755.0251	308.9227	10545.93	6.9343

4.3 Engine Comparisons

As previously mentioned, firstly a result comparison will be made between an already studied turbofan engine and a turbofan model that would represent the "Turbofan" mode of the FLADE added. This is done in order to have a valid a engine model. After a valid model is established its "Extended Range" mode and "Turbofan" mode will be compared.

4.3.1 Comparison of Turbofan Model and Reference Engine

The turbofan model has been based on a previously studied engine. This is done to have a validated the model. More specifically, the same mission as used in the reference study has been used here. In table 4.3 temperature and pressure for the engine can be seen along with the thrust generated, thermal efficiency and propulsive efficiency. When compared with the results of the reference case in figure B.1 it can be seen that both results match quite nicely. It should be mentioned that in figure B.1 the bottom half represents the HPT power extraction case. Therefore it should be neglected for this particular study. By setting up matching models the claim of having a realistic turbofan model is directly validated.

Table 4.3: Performance and efficiency results for turbofan simulation

ALT (m)	M_0	P_{02} (kPa)	T_2 (K)	W_2 (kg/s)	P_{03} (K)	T_3 (K)	P_{04} (kPa)	T_4 (K)	P_{05} (kPa)	T_5 (K)	F_N (kN)	η_e	η_p
0	0	90.18	288.15	90	2706.1	813.63	2597.8	1950	487.1	1260	79.3	0.432	0.0
610	0	84.21	284.19	79.02	2285.5	781.35	2192.9	1862	414.5	1199.6	66.0	0.425	0.0
610	0.1	86.43	284.75	87.67	2633.2	808.68	2528	1941	473	1252.9	110.7	0.241	0.054
610	0.18	90.48	286.03	90.54	2706.9	807.39	2598.5	1935.5	487	1249.4	112.9	0.246	0.095
610	0.44	104.25	295.2	103.77	3167.2	834.45	3041.1	2000.1	569.6	1296.2	127.0	0.270	0.209
2743	0.78	105.32	302.85	88.96	3370.2	879.25	3235.2	2078.4	668.9	1382.9	113.2	0.340	0.299
7010	0.88	65.54	279.83	65.85	1939	789.89	1861.1	1894.4	348.3	1219.6	78.9	0.310	0.331
9144	0.9	50.4	265.87	30.13	663.6	603.33	634.2	1362.7	127.2	872.9	12.4	0.429	0.574
9144	1.6	115.12	346.15	89.16	2737.2	903.55	2627.4	2122.4	504.1	1396.9	101.0	0.377	0.460
9144	0.9	49.7	265.87	45.91	1253.6	721.92	1202.1	1718.3	227.2	1098.6	53.2	0.292	0.340
9144	1.56	110.22	340.35	79.56	2336.2	864.18	2241	2019.4	433.6	1323.7	89.1	0.360	0.464

4.3.2 Range Extended Turbofan mode vs Turbofan Mode

After the turbofan model had been validated, the FLADE was added to the model and the model has then been configured for the Extended Range Mode. The performance results and the efficiencies of the Extended Range Turbofan model are as presented in the table 4.4.

Table 4.4: Performance and efficiency results for Extended Range Turbofan simulation

ALT (m)	M_0	P_2 (kPa)	T_2 (K)	W_2 (kg/s)	P_{03} (K)	T_3 (K)	P_{04} (kPa)	T_4 (K)	P_{05} (kPa)	T_5 (K)	F_N (kN)	η_e	η_p
0	0	90.18	288.15	90	2706.1	813.63	2598	1950	472.3	1251.9	74	0.439	0
610	0	83.99	284.19	82.26	2426.7	795.36	2329	1902.9	424.7	1219.1	66	0.437	0
610	0.1	85.97	284.75	91.45	2837.1	831.06	2725	2005.2	489.7	1288.5	109.3	0.268	0.054
610	0.18	89.82	286.03	95.29	2960.6	833.99	2844	2011.7	511.1	1293.4	112.9	0.274	0.095
610	0.44	103.9	295.2	108.59	3428.2	858.13	3293	2067.1	592.5	1334.3	125.3	0.296	0.209
2743	0.78	104.1	302.85	107.42	3436.4	878.28	3302	2112.7	594.4	1368.4	121.1	0.33	0.315
7010	0.88	65.26	279.83	70.04	2153.7	819.1	2068	1977.7	371	1268.2	78.7	0.336	0.329
9144	0.9	50.34	265.87	31.84	707.3	615.32	676.3	1398.7	131.7	891.4	12.4	0.438	0.569
9144	1.6	114.6	346.15	96.74	3079.3	932.77	2958	2201	545.6	1444.5	101	0.402	0.455
9144	0.9	49.52	265.87	49.04	1381.1	742.42	1325	1776.4	241.1	1129.4	53.2	0.316	0.338
9144	2	182.6	412.21	109.68	3359.8	988.41	3224	2260	619.7	1510.2	103.5	0.396	0.524

It is obvious that neither the performance nor the efficiency of the engine has changed noticeably. Both the thermal and propulsive efficiencies have been plotted as in the figure 4.6. In the figure it is shown that the propulsive and thermal efficiency of the Extended Range mode has slightly higher values at almost all of the points. However, in terms of propulsive efficiency both configurations models are almost the same, if not exactly the same throughout the simulation. The exception being point 7, which as mentioned is an important point for the simulation.

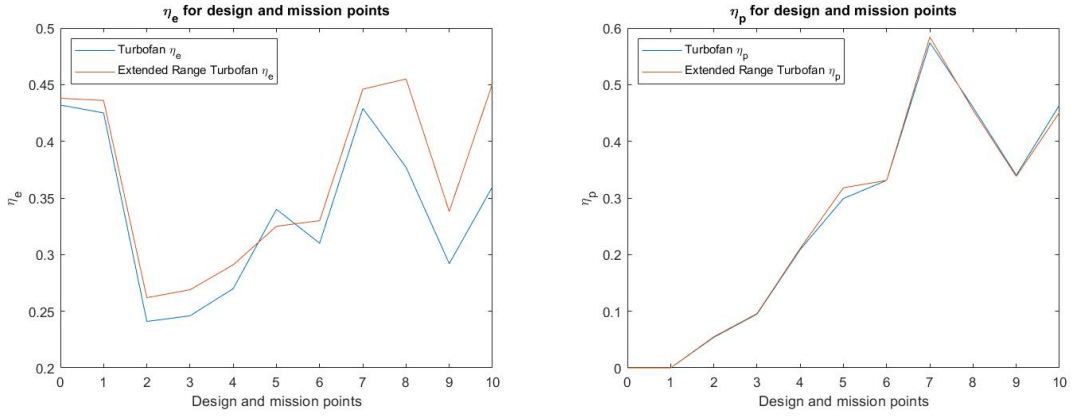

(A) (B)

Figure 4.6: η_e (A) and η_p (B) values for both Turbofan and Extended Range Model at design point (Point 0) and mission points

4.3.3 Cruise Performance

As mentioned in the section 3.4 a cruise analysis has been done with with M_0 and net thrust requirements from table 3.3. However, as seen from the results of the FLADE analysis in section 4.2 the kinetic energy contribution of the FLADE is not very substantial. Thus, it has raised the question of "How would changing the BPR1 (FLADE stream BPR) value affect the range?". For this analysis the Breguet Range equation, expressed by equation (2.26) has been used. In the equation the weight (and also F_L) and the gravity g would not be changed with changing the flight M_0

and thus the thrust. Therefore the range will be compared with η_o/F_D only. Range results for changing BPR1 without changing any of the engine limitations are as in table 4.5. Also net thrust produced by the engine is given in table 4.6.

Table 4.5: Change of η_o/F_D with change of BPR1 (FLADE bypass ratio)

M0	BPR1 1.7	BPR1 1.5	BPR1 1.25	BPR1 1.0	BPR1 0.9	BPR1 0.8	BPR1 0.7	BPR1 0.6	BPR1 0.5
DP	0.00E+00	0.00E+00	0.00E+00	0.00E+00	0.00E+00	0.00E+00	0.00E+00	0.00E+00	0.00E+00
0.45	1.28E-02	1.18E-02	1.06E-02	9.50E-03	9.04E-03	8.59E-03	8.35E-03	7.63E-03	8.24E-03
0.5	1.36E-02	1.27E-02	1.13E-02	1.01E-02	9.64E-03	9.15E-03	8.72E-03	8.66E-03	8.63E-03
0.55	1.44E-02	1.33E-02	1.20E-02	1.07E-02	1.02E-02	9.62E-03	9.13E-03	8.96E-03	8.93E-03
0.6	1.50E-02	1.40E-02	1.25E-02	1.11E-02	1.06E-02	1.01E-02	9.49E-03	9.18E-03	9.15E-03
0.65	1.55E-02	1.43E-02	1.29E-02	1.15E-02	1.10E-02	1.03E-02	9.77E-03	9.32E-03	9.27E-03
0.7	1.58E-02	1.47E-02	1.32E-02	1.17E-02	1.12E-02	1.06E-02	1.00E-02	9.44E-03	9.29E-03
0.75	1.60E-02	1.49E-02	1.34E-02	1.19E-02	1.13E-02	1.07E-02	1.01E-02	9.56E-03	9.09E-03
0.8	1.61E-02	1.49E-02	1.34E-02	1.20E-02	1.14E-02	1.08E-02	1.02E-02	9.63E-03	9.01E-03
0.85	1.61E-02	1.49E-02	1.34E-02	1.20E-02	1.14E-02	1.08E-02	1.02E-02	9.61E-03	9.01E-03
0.9	1.60E-02	1.48E-02	1.33E-02	1.19E-02	1.12E-02	1.07E-02	1.01E-02	9.53E-03	8.92E-03

M0	BPR1 0.4	BPR1 0.3	BPR1 0.2	BPR1 0.1	TF
DP	0.00E+00	0.00E+00	0.00E+00	0.00E+00	0.00E+00
0.45	8.17E-03	6.20E-03	7.99E-03	7.89E-03	7.71E-03
0.5	8.54E-03	8.43E-03	8.35E-03	8.27E-03	8.10E-03
0.55	8.87E-03	8.78E-03	8.70E-03	8.61E-03	8.43E-03
0.6	9.10E-03	9.02E-03	8.94E-03	8.87E-03	8.71E-03
0.65	9.25E-03	9.17E-03	9.11E-03	9.03E-03	8.20E-03
0.7	9.26E-03	9.20E-03	9.14E-03	9.07E-03	8.91E-03
0.75	9.09E-03	9.05E-03	8.99E-03	8.94E-03	8.80E-03
0.8	8.74E-03	8.72E-03	8.70E-03	8.65E-03	8.54E-03
0.85	8.41E-03	8.21E-03	8.23E-03	8.20E-03	8.11E-03
0.9	8.33E-03	7.78E-03	7.43E-03	7.47E-03	7.39E-03

Table 4.6: Change of net thrust with change of BPR1 (FLADE bypass ratio)

M0	BPR1 1.7	BPR1 1.5	BPR1 1.25	BPR1 1.0	BPR1 0.9	BPR1 0.8	BPR1 0.7	BPR1 0.6	BPR1 0.5	BPR1 0.4	BPR1 0.3	BPR1 0.2	BPR1 0.1	TF
0.45	13.7	14.5	15.6	16.9	17.5	18.2	18.5	19.9	18.5	18.5	23.3	18.5	18.5	18.5
0.5	13.9	14.6	15.8	17.2	17.8	18.5	19.2	19.2	19.2	19.2	19.2	19.2	19.2	19.2
0.55	14.1	14.9	16	17.5	18.1	18.9	19.7	19.9	19.9	19.9	19.9	19.9	19.9	19.9
0.6	14.3	15.1	16.4	17.9	18.6	19.3	20.2	20.7	20.7	20.7	20.7	20.7	20.7	20.7
0.65	14.6	15.5	16.8	18.3	19	19.9	20.8	21.6	21.6	21.6	21.6	21.6	21.6	21.6
0.7	15	15.9	17.2	18.9	19.6	20.5	21.4	22.4	22.7	22.7	22.7	22.7	22.7	22.7
0.75	15.5	16.4	17.8	19.5	20.3	21.2	22.2	23.2	24.2	24.2	24.2	24.2	24.2	24.2
0.8	16	17	18.5	20.2	21.1	22	23	24.1	25.4	26.1	26.1	26.1	26.1	26.1
0.85	16.6	17.7	19.2	21	21.9	22.9	23.9	25.1	26.5	28	28.6	28.6	28.6	28.6
0.9	17.3	18.4	20	21.9	22.9	23.9	25	26.2	27.7	29.3	31.1	32.3	32.3	32.3

Table 4.5 shows significant improvement of the range with the increase of the BPR1. However, when checked with table 4.6 it can be seen that after BPR1=0.2 the engine is not able to meet the thrust requirements. This is more evident in figure 4.7 and 4.8, especially in the figure 4.8 where all the thrust values from all the BPR1 values should have been the exactly same.

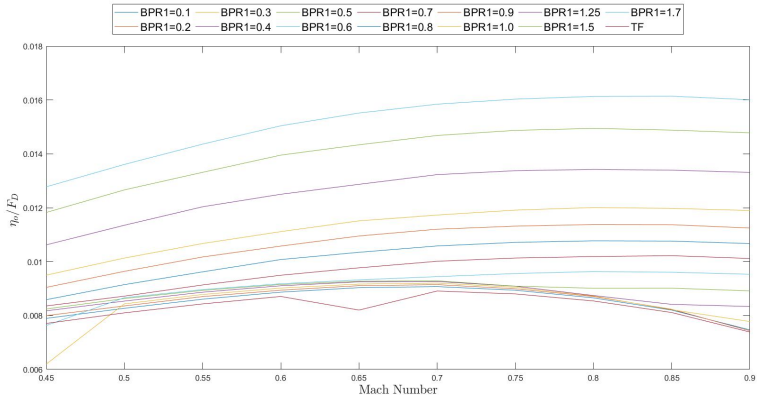

Figure 4.7: Effect of BPR1 on η_o/D at different cruise M_0

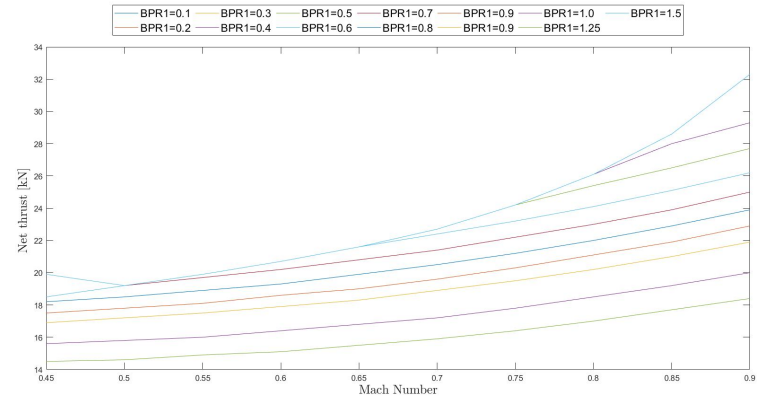

Figure 4.8: Net thrust [kN] with different BPR1 values at different cruise M_0

After these results were obtained there were some possible options that could have been studied further. These are; increasing the mass flow through the engine and/or increasing the OPR and max turbine inlet temperature. However, increasing the mass flow would essentially result in a different engine size. The drag figures would then have to be adjusted for the new mass flow. Therefore these study options have been pursued. A new set of analysis have been done with increasing the OPR and TIT so the engine would satisfy the thrust requirements. From within GESTPAN, OPR and TIT limits have been raised from 33 and $2260K$ to 50 and $2400K$ respectively. Also, the maximum cruise Mach number has been lowered to $M = 0.75$ since the higher the Mach number, the lower the FLADE stream efficiency and kinetic energy. The range and net thrust results[1] for the revised analysis are in tables 4.7 and 4.8 respectively.

[1] 0's in the tables (Other than the η_o/F_D results at DP) represent the failed off-design points

Table 4.7: Change of η_o/F_D with change of BPR1 (FLADE bypass ratio) without limiting factors

M0	BPR1 0.1	BPR1 0.2	BPR1 0.3	BPR1 0.4	BPR1 0.5	BPR1 0.6	BPR1 0.7	BPR1 0.8	BPR1 0.9
DP	0.00E+00	0.00E+00	0.00E+00	0.00E+00	0.00E+00	0.00E+00	0.00E+00	0.00E+00	0.00E+00
0.45	7.89E-03	7.99E-03	8.07E-03	8.17E-03	8.24E-03	8.29E-03	8.35E-03	8.40E-03	8.44E-03
0.5	8.27E-03	8.35E-03	8.43E-03	8.54E-03	8.63E-03	8.66E-03	8.72E-03	8.73E-03	8.77E-03
0.55	8.61E-03	8.70E-03	8.78E-03	8.87E-03	8.93E-03	8.96E-03	9.02E-03	9.03E-03	9.05E-03
0.6	8.87E-03	8.94E-03	9.02E-03	9.10E-03	9.15E-03	9.18E-03	9.19E-03	9.22E-03	9.19E-03
0.65	9.03E-03	9.11E-03	9.17E-03	9.25E-03	9.27E-03	9.32E-03	9.33E-03	9.32E-03	9.29E-03
0.7	9.07E-03	9.14E-03	9.20E-03	9.26E-03	9.29E-03	9.30E-03	9.30E-03	9.29E-03	9.20E-03
0.75	8.94E-03	8.99E-03	9.05E-03	9.09E-03	9.09E-03	9.10E-03	9.08E-03	8.97E-03	8.89E-03
0.8	8.65E-03	8.70E-03	8.72E-03	8.74E-03	8.73E-03	8.70E-03	8.63E-03	8.53E-03	8.37E-03
0.85	8.20E-03	8.23E-03	8.21E-03	8.20E-03	8.17E-03	8.06E-03	7.95E-03	7.76E-03	7.57E-03
0.9	7.47E-03	7.43E-03	7.39E-03	7.35E-03	7.20E-03	7.03E-03	6.82E-03	6.54E-03	6.21E-03

M0	BPR1 1.0	BPR1 1.1	BPR1 1.2	BPR1 1.3	BPR1 1.4	TF
DP	0.00E+00	0.00E+00	0.00E+00	0.00E+00	0.00E+00	0.00E+00
0.45	8.46E-03	8.44E-03	8.40E-03	8.34E-03	8.25E-03	7.71E-03
0.5	8.75E-03	8.70E-03	8.66E-03	8.57E-03	8.49E-03	8.10E-03
0.55	9.02E-03	8.97E-03	8.88E-03	8.77E-03	8.66E-03	8.43E-03
0.6	9.14E-03	9.07E-03	8.94E-03	8.83E-03	8.68E-03	8.71E-03
0.65	9.20E-03	9.13E-03	8.99E-03	8.84E-03	8.67E-03	8.20E-03
0.7	9.11E-03	8.98E-03	8.83E-03	8.66E-03	8.47E-03	8.91E-03
0.75	8.76E-03	8.58E-03	8.40E-03	8.18E-03	7.91E-03	8.80E-03
0.8	8.20E-03	8.00E-03	7.72E-03	7.56E-03	0.00E+00	8.54E-03
0.85	7.30E-03	7.00E-03	7.05E-03	0.00E+00	0.00E+00	8.11E-03
0.9	6.36E-03	0.00E+00	0.00E+00	0.00E+00	0.00E+00	7.39E-03

Table 4.8: Change of net thrust with change of BPR1 (FLADE bypass ratio) without limiting factors

M0	BPR 0.1	BPR 0.2	BPR 0.3	BPR 0.4	BPR 0.5	BPR 0.6	BPR 0.7	BPR 0.8	BPR 0.9	BPR 1.0	BPR 1.1	BPR 1.2	BPR 1.3	BPR 1.4	TF
DP	74	69.6	65.8	62.5	59.7	57.2	55	53	51.2	49.6	48.2	46.8	45.6	44.5	79.4
0.45	18.5	18.5	18.5	18.5	18.5	18.5	18.5	18.5	18.5	18.5	18.5	18.5	18.5	18.5	18.5
0.5	19.2	19.2	19.2	19.2	19.2	19.2	19.2	19.2	19.2	19.2	19.2	19.2	19.2	19.2	19.2
0.55	19.9	19.9	19.9	19.9	19.9	19.9	19.9	19.9	19.9	19.9	19.9	19.9	19.9	19.9	19.9
0.6	20.7	20.7	20.7	20.7	20.7	20.7	20.7	20.7	20.7	20.7	20.7	20.7	20.7	20.7	20.7
0.65	21.6	21.6	21.6	21.6	21.6	21.6	21.6	21.6	21.6	21.6	21.6	21.6	21.6	21.6	21.6
0.7	22.7	22.7	22.7	22.7	22.7	22.7	22.7	22.7	22.7	22.7	22.7	22.7	22.7	22.7	22.7
0.75	24.2	24.2	24.2	24.2	24.2	24.2	24.2	24.2	24.2	24.2	24.2	24.2	24.2	24.2	24.2
0.8	26.1	26.1	26.1	26.1	26.1	26.1	26.1	26.1	26.1	26.1	26.1	26.1	25.9	0	26.1
0.85	28.6	28.6	28.6	28.6	28.6	28.6	28.6	28.6	28.6	28.6	28.6	27.7	0	0	28.6
0.9	32.3	32.3	32.3	32.3	32.3	32.3	32.3	32.3	32.3	31	0	0	0	0	32.3

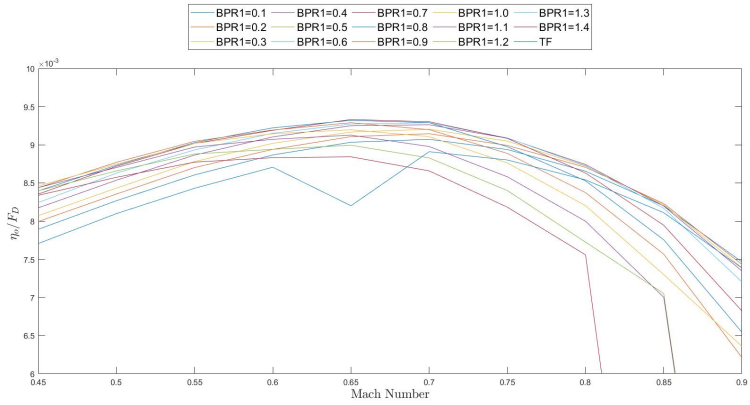

Figure 4.9: Affect of BPR1 on η_o/D at different cruise M_0 without limiting factors

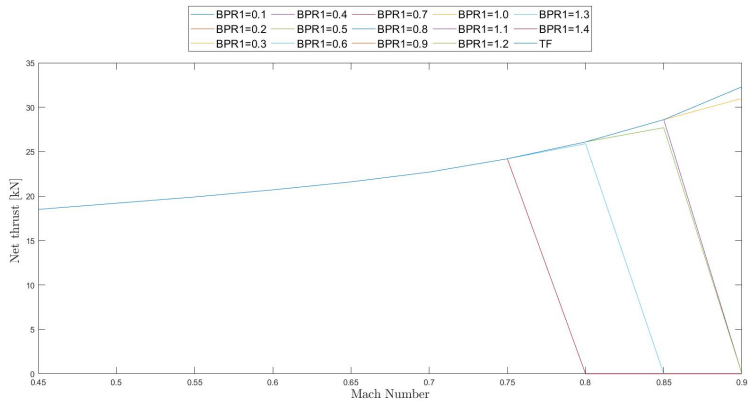

Figure 4.10: Net thrust[kN] with different BPR1 values at different cruise M_0 without limiting factors

These new results show that the BPR1=0.7 point reaches the highest η_o/F_D value. Thus it provides the longest range among the tried engine configurations. Also, as it could have been expected from the results of section 4.2 the best flight velocity for the cruise case would be around $M_0 = 0.7$. The contribution of the FLADE in a cruise situation have an inverse relation with the flight velocity. Thus at high speeds the FLADE only uses valuable torque from the low-pressure shaft without providing considerable thrust. With the addition of the FLADE at cruise level 9144 m and $M_0 = 0.7$ a range improvement of around 5% can be expected.

5

Conclusion and Future Work

5.1 Conclusion

There are three sets of conclusions related to this study each corresponding to sections 4.1, 4.2 and 4.3. The first set of conclusions revolve around explaining which factors should be taken into consideration and how they can contribute to make some safe design decisions for a choke-free off-design performance of the FLADE. The second set relates to validating the turbofan model used with a previously studied engine and more importantly comparing the turbofan model with the extended range model to see the changes from additions of the FLADE. Lastly, the final set of observations will be drawn studying the FLADE stream itself in terms of its efficiency and kinetic energy.

From the results in the section 4.1 following conclusions can be stated;

- Altitude and FPR are two main factors that decide if the FLADE stream will be choked or not.
- Having a low FPR ratio does not only reduce the energy of the stream but makes it more inclined to choking.
- Altitude plays a key role to whether the stream will be choked or not. The off-design point gets closer to choking up until around 9500 m. Then, due to ambient temperature being constant until 20000 m the points gets further away from choking. Thus, choking seems most likely to occur around 9500 m.
- Decrease of the Mach number moves the off-design point away from choking which can be anticipated fairly easily. However the effects are not as pronounced as for the altitude and FPR cases.

Reflecting on these conclusions it can be said that FPR should be set as high as possible for both performance and off-design performance of the FLADE. Also, having an off-design point around 9500 m where the engine will be throttled can be a nice way to see if there will be any choking which can also result in spillage drag.

Results form section 4.2 points out that;

- The polytropic efficiency of the FLADE over the mission and cruise analysis is quite close to the design efficiency.
- Also, it was expected that the FLADE stream would not have a major kinetic energy contribution. This is due to that the thrust contribution is proportionally small for a quite small BPR1 and consequently the mass flow through the duct is then small.
- Cruise analysis isolated the FLADE performance and velocity relation. It has been shown that with the increase of the cruise Mach number the kinetic energy contribution of the FLADE is reducing drastically. This is due to that the FLADE stream reaches a maximum exhaust velocity at $M = 1$. In order to produce thrust there needs to be a velocity difference between flight velocity and jet velocity. Thus, the kinetic energy from the FLADE stream diminishes with the increase of the flight velocity.

It has been observed that the FLADE polytropic efficiency is high through both the mission and the cruise analysis. However the cruise analysis show that the contribution of the FLADE stream reduces with the increase of the Mach number. Thus, a FLADE assisted cruise should not be conducted at high subsonic range ($M > 0.85$) particularly without a convergent-divergent nozzle that can turn the subsonic stream into a supersonic one.

By the results from section 4.3 the following can be said;

- The turbofan model compares well with the engine from the reference case, which validates the engine model used as a realistic and applicable engine.

- Having the FLADE and a separate stream did not change the engine performance considerably neither towards better or worse. Thermal efficiency of the extended range model is slightly better than the turbofan at almost every mission point. Contrary to the thermal efficiency, the propulsive efficiency of the extended range model is almost exactly the same as for the turbofan model. This refers to the total propulsive efficiency and not to the propulsive efficiency of the individual nozzle streams. Such a result must be expected for BPR1=0.1, for which the FLADE does not provide a considerable amount of thrust and the mass flow through the engine is 10/11 of the original turbofan model.

- The first cruise analysis showed that simply increasing the bypass ratio will not be very effective and engine will not produce the thrust required from it, due to the OPR and TIT limitations set within the performance model. From these results it have been seen that to operate the FLADE at a higher BPR the engine needs to have headroom to increase the OPR and TIT.

- With the limitations increased to give the engine some headroom the thrust reached the targeted levels. The results show that even with sufficient headroom for all the points, the BPR1=0.7 design seems to yield the best range

results, with a possible increase in range of 5% over the turbofan engine from the reference case.

From these conclusion it can be said that, in terms of raw performance the extended range model is not considerably better than the turbofan model due to the small BPR1. Directly increasing the ratio may end up in the engine reaching the OPR and the TIT limits, therefore before increasing the BPR it should be checked if the engine is operating close to the limit or if it has some headroom. Given properly high OPR and TIT as limits $BPR1 = 0.7$ gave the best range results with noticeable improvements over the turbofan engine.

5.2 Future Work

Possible future work for this project could include;

- Developing a weight model for the engine to assess the effect of the addition of the FLADE on the engine weight.
- The addition of the FLADE to a double bypass ACE engine, exploring the possibility of having a variable geometry FLADE stage.
- A two-stage FLADE to have a higher pressure ratio for higher cruise speeds, possibly in combination with a convergent-divergent FLADE nozzle.
- One of the trademarks of the FLADE is the possible improvement in the engine cooling. The stream could be used to have a cooler turbine cooling air by integrating a heat exchanger, thereby allowing an increase in the TIT.

Bibliography

[1] Randle, A., 2021. History of flight: Breakthroughs, disasters and more. History.com. Available at: https://www.history.com/news/history-flight-aviation-timeline [Accessed April 14, 2022].

[2] Greicius, T., 2021. The wright brothers. NASA. Available at: https://www.nasa.gov/image-feature/jpl/the-wright-brothers [Accessed April 14, 2022].

[3] Anon, Chaper 3 Jet Propulsion: Too Little, Too Late. NASA. Available at: https://history.nasa.gov/SP-4306/ch3.htm [Accessed April 14, 2022].

[4] Anon, 2007. The jet engine 5th ed., London: Rolls-Royce plc.

[5] Anon, 2022. What are the advantages and disadvantages of turboprop engines? National Aviation Academy. Available at: https://www.naa.edu/advantages-and-disadvantages-of-turboprop-engines/ [Accessed April 14, 2022].

[6] Simmons, R.J., 2009. Design and control of a variable geometry turbofan with and independently modulated third stream (Doctoral dissertation, The Ohio State University).

[7] Johnson, J.E., Foster, T. amp; Allan, R.D., 1977. VARIABLE CYCLE GAS TURBINE ENGINES .

[8] Reim, G., 2021. USAF prepares to test adaptive engines from GE, Pamp;W. Flight Global. Available at: https://www.flightglobal.com/fixed-wing/usaf-prepares-to-test-adaptive-engines-from-ge-pandw/145613.article [Accessed April 15, 2022].

[9] Wadia, A.R., Turner, A.G., Dziech, A.M., Szucs, P.N. and Decker, J.J., General Electric Co, 2010. FLADE fan with different inner and outer airfoil stagger angles at a shroud therebetween. U.S. Patent 7,758,303.

[10] Wadia, A.R. et al., 2010. FLADE FAN WITH DIFFERET INNER AND OUTER AIRFOIL STAGGER ANGELS AT A SHORUD THERE BETWEEN. European Patent 1895142A2

[11] Saravanamuttoo, H.I., Rogers, G.F.C. and Cohen, H., 2001. Gas turbine theory(6th edition). Pearson Education.

[12] Anderson, J.D., 2021. Modern compressible flow: With historical perspective, New York: McGraw Hill.

[13] Spakovszky, Z.S. amp; Waitz, I.A., 2022. Thermodynamics and Propulsion. Aircraft Range: the Breguet Rabge Equation.

[14] Anon, Aeolus: Introduction. JetX Engineering. Available at: https://www.jet-x.org/a1.html [Accessed May 9, 2022].

[15] IV, P.R.K., SR-71 Flight Manual. SR. Available at: https://www.sr-71.org/blackbird/manual/1/1-33.php [Accessed April 20, 2022].

[16] Willis, E.A. and Welliver, A.D., 1976, January. Supersonic variable-cycle engines. In Propulsion Conf. (No. NASA-TM-X-73524).
[17] Powers, A.G., Whitlow, J.B. and Stitt, L.E., 1976, January. Component test program for variable-cycle engines. In Proc. of the SCAR Conf., Part 1.
[18] Howlett, R.A., 1975. Advanced supersonic propulsion study, phase 2 (No. NASA-CR-134904).
[19] Westmoreland, J.S., 1980. Progress with variable cycle engines. NASA. Langley Research Center Supersonic Cruise Res. 1979, Pt. 1.
[20] Thomas, W.W. and Sprunger, E.V., 1977. Two spool variable cycle engine. U.S. Patent 4,043,121
[21] Johnson, J.E. and General Electric Co, 1995. Spillage drag and infrared reducing FLADE engine. U.S. Patent 5,404,713.
[22] Ciokajlo, J.J. and O'Brein, M.T., 1995. Hybrid rotor blade. U.S. Patent 5,388,964A
[23] Buettner, R.W., 2017. Dynamic Modeling and Simulation of a Variable Cycle Turbofan Engine with Controls.
[24] Johnson, J.E. and Powell, B.F., 2011. Adaptive engine. U.S. Patent 20,110,167,792
[25] Lyu, Y., Tang, H. and Chen, M., 2016. A study on combined variable geometries regulation of adaptive cycle engine during throttling. Applied Sciences, 6(12), p.374.
[26] Buettner, R.W., 2017. Dynamic Modeling and Simulation of a Variable Cycle Turbofan Engine with Controls.
[27] Nascimento, M.A.R., 1992. The selective bleed variable cycle engine (Doctoral dissertation, Cranfield Institute of Technology).
[28] Wood, A. and Pilidis, P., 1997. A variable cycle jet engine for ASTOVL aircraft. Aircraft Engineering and Aerospace Technology.
[29] Grönstedt, T., 2000. Development of methods for analysis and optimization of complex jet engine systems. Chalmers Tekniska Hogskola (Sweden).
[30] Grönstedt UT, Pilidis P. Control optimization of the transient performance of the selective bleed variable cycle engine during mode transition. J. Eng. Gas Turbines Power. 2002 Jan 1;124(1):75-81.
[31] Rosell, D. and Grönstedt, T., 2022. Design Considerations of Low Bypass Ratio Mixed Flow Turbofan Engines with Large Power Extraction. Fluids, 7(1), p.21.

A

Appendix 1

A.1 ISA Tables

Table A.1: International Standard Atmosphere Table

Elevation **-z-** **(m)**	**Temperature** **-T-** **(K)**	**Pressure** **-p-** **(bar)**	**Relative Density** **-ρ/ρ_o-** **(kg/m^3)**	**Speed of sound** **-c-** **(m/s)**
-2000	301.2	1.2778	1.2067	347.9
-1500	297.9	1.2070	1.1522	346.0
-1000	294.7	1.1393	1.0996	344.1
-500	291.4	1.0748	1.0489	342.2
0	288.15	1.01325	1.0000	340.3
500	284.9	0.9546	0.9529	338.4
1000	281.7	0.8988	0.9075	336.4
1500	278.4	0.8456	0.8638	334.5
2000	275.2	0.7950	0.8217	332.5
2500	271.9	0.7469	0.7812	330.6
3000	268.7	0.7012	0.7423	328.6
3500	265.4	0.6578	0.7048	326.6
4000	262.2	0.6166	0.6689	324.6
4500	258.9	0.5775	0.6343	322.6
5000	255.7	0.5405	0.6012	320.5
5500	252.4	0.5054	0.5694	318.5
6000	249.2	0.4722	0.5389	316.5
6500	245.9	0.4408	0.5096	314.4
7000	242.7	0.4111	0.4817	312.3
7500	239.5	0.3830	0.4549	310.2
8000	236.2	0.3565	0.4292	308.1
8500	233.0	0.3315	0.4047	306.0
9000	229.7	0.3080	0.3813	303.8
9500	226.5	0.2858	0.3589	301.7
10000	223.3	0.2650	0.3376	299.8

Elevation -z- (m)	**Temperature** -T- (K)	**Pressure** -p- (bar)	**Relative Density** -ρ/ρ_o- (kG/m^3)	**Speed of sound** -c- (m/s)
10500	220.0	0.2454	0.3172	297.4
11000	216.8	0.2270	0.2978	295.2
11500	216.7	0.2098	0.2755	295.1
12000	216.7	0.1940	0.2546	295.1
12500	216.7	0.1793	0.2354	295.1
13000	216.7	0.1658	0.2176	295.1
13500	216.7	0.1533	0.2012	295.1
14000	216.7	0.1417	0.1860	295.1
14500	216.7	0.1310	0.1720	295.1
15000	216.7	0.1211	0.1590	295.1
15500	216.7	0.1120	0.1470	295.1
16000	216.7	0.1035	0.1359	295.1
16500	216.7	0.09572	0.1256	295.1
17000	216.7	0.08850	0.1162	295.1
17500	216.7	0.08182	0.1074	295.1
18000	216.7	0.07565	0.09930	295.1
18500	216.7	0.06995	0.09182	295.1
19000	216.7	0.06467	0.08489	295.1
19500	216.7	0.05980	0.07850	295.1
20000	216.7	0.05529	0.07258	295.1
22000	218.6	0.04047	0.05266	296.4
24000	220.6	0.02972	0.03832	297.7
26000	222.5	0.02188	0.02797	299.1
28000	224.5	0.01616	0.02047	300.4
30000	226.5	0.01197	0.01503	301.7

A.2 Fuel-Air Ratio Chart

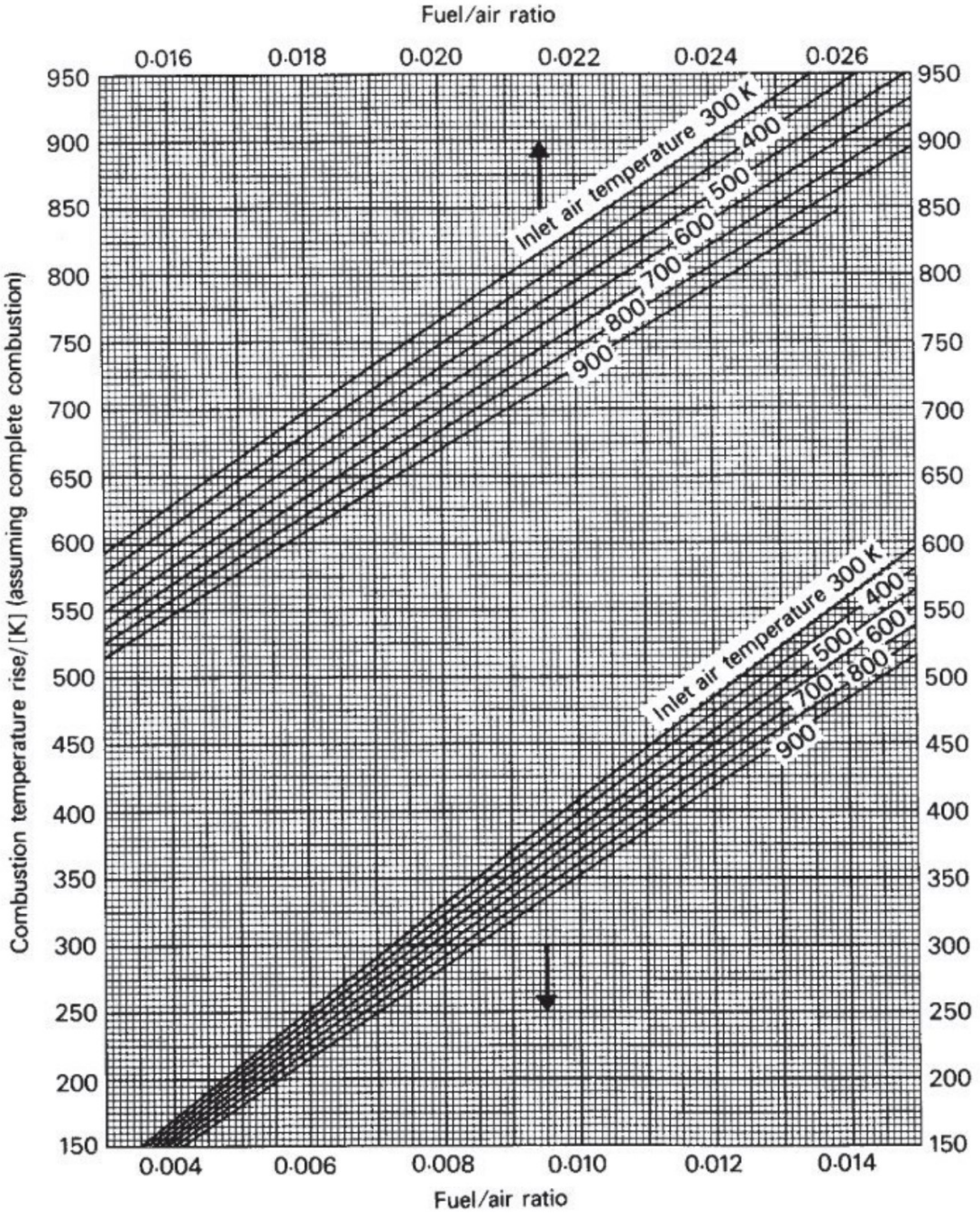

Figure A.1: Air-fuel ratio chart [11]

B

Appendix 2

B.1 Results From Reference Case

ALT	M_0	P_{T0}	P_{T2}	T_2	W_2	BPR	P_{T3}	T_3	P_{T4}	T_4	P_{HPT}	P_{T45}	T_{45}	P_{LPT}	P_{T5}	T_5	P_{T8}	T_8	F_N	η_{th}	η_p
[m]	-	[kPa]	[kPa]	[K]	[kg/s]	-	[kPa]	[K]	[kPa]	[K]	[kW]	[kPa]	[K]	[kW]	[kPa]	[K]	[kPa]	[K]	[kN]	-	-
610	0.0	94.2	84.2	284	78.9	0.468	2280	782	2190	1870	0	901	1410	0	415	1200	410	991	66	0.42	0
610	0.1	94.9	86.4	285	87.6	0.447	2630	808	2530	1940	0	1040	1470	0	473	1250	399	2090	111	0.24	0.05
610	0.18	96.4	90.5	286	90.4	0.452	2700	807	2600	1930	0	1070	1470	0	487	1250	411	2090	113	0.25	0.1
610	0.44	108	104	295	104	0.449	3170	835	3050	2000	0	1250	1520	0	570	1300	489	2090	127	0.27	0.21
3048	0.775	108	104	303	105	0.44	3290	865	3160	2070	0	1300	1580	0	590	1350	514	2100	128	0.31	0.31
7010	0.875	67.4	65.5	280	65.7	0.455	1940	790	1860	1890	0	763	1440	0	348	1220	294	2080	78.9	0.31	0.33
9144	0.9	50.9	50.4	266	30	0.633	657	602	628	1370	0	257	1020	0	128	881	128	696	12.4	0.43	0.57
9144	1.6	127	115	346	88.7	0.498	2720	902	2610	2120	0	1080	1630	0	502	1400	441	2120	101	0.38	0.46
9144	0.9	50.8	49.7	266	45.8	0.485	1250	722	1200	1720	0	492	1290	0	227	1100	193	2060	53.2	0.29	0.34
9144	2.0	235	183	412	108	0.552	3320	985	3190	2260	0	1320	1750	0	634	1520	571	2130	113	0.38	0.52
610	0.0	94.2	84.3	284	77.7	0.496	2250	779	2170	1930	900	889	1460	0	415	1250	410	1020	66	0.42	0
610	0.1	94.9	86.5	285	87.1	0.47	2620	808	2520	2000	900	1040	1520	0	476	1300	408	2080	111	0.25	0.05
610	0.18	96.4	90.6	286	90	0.473	2700	807	2600	2000	900	1070	1520	0	491	1290	419	2080	113	0.25	0.09
610	0.44	108	104	295	103	0.467	3170	835	3050	2050	900	1250	1560	0	575	1340	498	2090	127	0.28	0.21
3048	0.775	108	104	303	105	0.456	3300	865	3170	2130	900	1300	1620	0	596	1390	524	2090	128	0.32	0.31
7010	0.875	67.4	65.6	280	65.5	0.484	1940	791	1870	1990	900	768	1510	0	354	1290	301	2080	78.9	0.32	0.33
9144	0.9	50.9	50.5	266	26.9	0.814	591	594	571	1680	900	233	1250	0	124	1100	124	801	12.4	0.43	0.55
9144	1.6	127	115	346	88.7	0.515	2740	905	2640	2190	900	1090	1680	0	511	1450	454	2110	101	0.38	0.46
9144	0.9	50.8	49.7	266	45.4	0.53	1260	725	1220	1870	900	498	1410	0	234	1210	199	2060	53.2	0.3	0.34
9144	2.0	235	183	412	101	0.589	3030	964	2910	2260	900	1200	1750	0	588	1520	529	2130	105	0.38	0.53

Figure B.1: Results from the reference case

DEPARTMENT OF MECHANICS AND MARITIME SCIENCES
CHALMERS UNIVERSITY OF TECHNOLOGY
Gothenburg, Sweden
www.chalmers.se

CHALMERS
UNIVERSITY OF TECHNOLOGY